4-16-2013

Development of a Mechanically-Stimulated Tissue-Specific Extracellular Matrix Coated Scaffold for Tendon/Bone Interface Engineering

Jared Owen Cooper

DEVELOPMENT OF A MECHANICALLY-STIMULATED TISSUE-SPECIFIC EXTRACELLULAR MATRIX COATED SCAFFOLD FOR TENDON/BONE INTERFACE ENGINEERING

By

Jared Owen Cooper

A Dissertation

Submitted in Partial Fulfillment of the

Requirements for the Degree of

Doctor of Philosophy

Major: Biomedical Engineering

The University of Memphis

May 2013

DEDICATION

To my family. Thank you for all of your support, without which, I could not have accomplished any of my achievements.

ACKNOWLEDGEMENTS

I would like to thank my advisor, Warren Haggard, for being a mentor and sharing his wisdom and experience with me. I am also grateful to all of my committee members for their guidance. To my lab mates and fellow BAM members, thank you for the stimulating discussions and many suggestions you imparted. I am especially grateful to fellow graduate student, Ben Reves, for his many discussions on, and distractions from, all things research.

ABSTRACT

Cooper, Jared Owen. Ph.D. The University of Memphis. May 2013. Development of a Mechanically-Stimulated Tissue-Specific Extracellular Matrix Coated Scaffold for Tendon/Bone Interface Engineering. Major Professor: Warren O. Haggard, Ph.D.

The enthesis is a complex anatomical and functional interface between tendon and bone. Once injured, this site does not readily heal and is repaired with limited success. To aid in repair of the enthesis a commercially available scaffold was chosen, from 3 candidate biomaterials, with fibroblast and osteoblast deposited extracellular matrix (ECM) to create a tendon and bone region, respectively, on the scaffold. To further enhance the ECM deposition, the seeded scaffold was mechanically stimulated in a custom built bioreactor for 35 days. The scaffolds were then evaluated by looking at tissue specific gene activation of mesenchymal stem cells (MSC)s due to the deposited ECM.

Out of the three materials, non-degradable polyester fabric (PET), degradable polylactic acid (PLA) fabric, and biologic acellular dermal matrix (ACDM), the PLA fabric had the best combination of ECM deposition and mechanical strength for the project. After selecting a scaffold, we determined the parameters for co-culture medium, with respect to fibroblast and osteoblast mineralization. It was determined that standard growth medium, alpha-MEM + 10% fetal bovine serum + 1000 U/mL penicillin, 1000 μg/mL streptomycin, 2.5 μg/mL amphotericin-B + 3 mM beta-glycerophosphate + 25 μg/mL of ascorbic acid provided low fibroblast mineralization while still allowing for osteoblast mineralization. Fluorescence imaging demonstrated that a co-cultured scaffold could be seeded to produce two distinct tissue specific regions. The transition zone produced had values for collagen and glycosaminoglycan (GAG) deposition between that

of the two tissue specific regions. Lastly after mechanical conditioning, stimulating the entire scaffold produced an increase in cell number, and the ratio of collagen to GAG in ECM compared to static culture. When the MSCs were exposed to the tissue specific regions, entirely stretched ECM caused an increase in collagen and tendon-specific GAG gene activation and a decrease in mineralization gene activation compared to tissue culture plastic. Cartilage specific markers were unchanged.

In conclusion, a suitable commercially available scaffold was identified. The scaffold was seeded so a tendon specific and bone specific regions were distributed on the scaffold. Mechanically conditioning the scaffolds in a bioreactor increased the activation of tissue specific genes for tendon and bone compared to stem cells seeded on tissue culture plastic. Future work includes a functional scaffold testing in an *in vivo* tendon-to-bone animal model.

PREFACE

This body of research was funded by a Department of Defense PRORP Grant, Award # W81XWH-10-1-0768 entitled “Enhanced soft tissue attachment and fixation using a mechanically-stimulated cytoselective tissue-specific ECM coating”. Outlined in this grant was the basis for the organization of the research performed here. The purpose of this research was to apply modern tissue engineering techniques with commercially available biomaterials to aid in repair of tendon-to-bone injuries. Many soft tissue injuries occur in the civilian realm; however with rising incidences of injured soldiers, the Army is interested in providing functional care to more quickly to rehabilitate these wounded warriors. The main body of this dissertation contains the following manuscripts which will be submitted for publication as noted:

Chapter 2: Scaffold Considerations for Tendon/Bone Interface Engineering. *Planned submission to Journal of Functional Biomaterials (APR 2013).*

Chapter 3: Co-Cultured Tissue Specific Scaffolds for Tendon/Bone Interface Engineering. *Planned submission to Journal of Orthopedic Research (APR 2013).*

Chapter 4: Mechanically-Stimulated Co-Cultured Tissue-Specific Scaffolds for Tendon/Bone Interface Engineering. Planned submission to *Journal of Biomedical Materials Research Part B: Applied Biomaterials (APR 2013).*

TABLE OF CONTENTS

CHAPTER		PAGE
List of Figures		ix
1	Introduction	1
	Anatomy and Problem	1
	Current Research Strategies	4
	Hypothesis	7
2	Scaffold Considerations for Tendon/Bone Interface Engineering	8
	Introduction	8
	Methods	10
	Results	16
	Discussion	25
	References	31
3	Co-cultured Tissue-Specific Scaffolds for Tendon/Bone Interface Engineering	35
	Introduction	35
	Methods	36
	Results	41
	Discussion	49
	References	54
4	Mechanically-Stimulated Co-cultured Tissue Specific Scaffolds for Tendon/Bone Interface Engineering	58
	Introduction	58
	Methods	60
	Results	67
	Discussion	76
	References	80
5	Planned *In Vivo* Animal Model	85
6	Conclusions	87
7	Recommendations for Future Work	89
References		90

LIST OF FIGURES

FIGURES		PAGE
Chapter 2. 1	SEM of candidate scaffolds	18
Chapter 2. 2	Image of live/dead staining on scaffolds	20
Chapter 2. 3	High magnification of live/dead stained scaffolds	21
Chapter 2. 4	Graph of DNA for MC 3T3 and NIH 3T3	22
Chapter 2. 5	Graph of GAG/DNA for MC 3T3 and NIH 3T3 cells	23
Chapter 2. 6	Graph of HYP/DNA for MC 3T3 and NIH 3T3 cells	24
Chapter 2. 7	BioTape characterization of HYP and GAG	25
Chapter 3. 1	Schematic of scaffold seeding	38
Chapter 3. 2	Graph of total protein deposition for medium determination	42
Chapter 3. 3	Graph of calcium deposition for medium determination	43
Chapter 3. 4	Fluorescent image of tissue specific regions on PLA	44
Chapter 3. 5	High magnification selections of tissue-specific regions on PLA scaffold	45
Chapter 3. 6	Fluorescent images of cell migration on PLA	46
Chapter 3. 7	Graph of DNA and ECM quantification for tissue-specific areas	48
Chapter 4. 1	Schematic of scaffold seeding	61
Chapter 4. 2	Mechanical bioreactor assembly	63
Chapter 4. 3	Graphs of MSC tissue specific gene activation	70
Chapter 4. 4	Graph of DNA and ECM quantification of stimulated scaffolds	72

Chapter 4. 5	Histological staining of FB STIM scaffolds	74
Chapter 4. 6	High magnification image of conditioned ECM coating	75
Chapter 4. 7	Histological staining of FB+OB STIM scaffolds	76

CHAPTER 1: INTRODUCTION

Anatomy and Problem

The enthesis (or tendon/ligament to bone interface) is a complex tissue interface that attaches tendon or ligament to bone[1]. This interface is a continuous transition from tendon or ligament, to non-mineralized fibrocartilage, to a mineralized fibrocartilage to bone[1-3]. The function of the enthesis is to transfer loads from tendon to bone, both of which have different mechanical properties[2,4]. Much of how the mechanical loads are transferred is due to the anatomical specificity of the tissue shown in Figure 1[4]. Tendon is comprised of highly aligned collagen fibers in the direction of mechanical loading[4,5]. Most of the tendon fibers are composed of collagen type I and type III as well as approximately 2-4% elastin[4-6]. There are also proteoglycans such as decorin and biglycan that act as crosslinkers within the tendon extracellular matrix (ECM) to aid in increased mechanical strength[4,7]. This ECM is maintained by specialized fibroblasts called tenocytes. Fibrocartilage is comprised of mostly collagen type II, with small amounts of collagen type III and less collagen type I and type X[4,5,7]. The collagen fibers become larger and alignment becomes less organized from tendon to fibrocartilage. Ovoid but aligned cells appear and there are higher amounts of aggrecan compared to other proteoglycans present in the fibrocartilage[4,8]. This layer transitions into mineralized fibrocartilage where round chondrocytes are present in a mineralizing matrix containing collagen type II and high amounts of collagen X and aggrecan[5,7]. The collagen matrix in the mineralizing region is much less organized than the fibrocartilage and tendon. Finally, bone is comprised of highly mineralized unaligned collagen type I matrix and no collagen type II[4]. This matrix is maintained and remodeled by osteoblasts, osteoclasts,

and osteocytes[7]. This gradual transition from highly aligned non-mineralized tendon to low alignment and high mineralization bone is important to relieve stress concentrations that could form between an abrupt transition from tendon to bone[5]. Even so, there are sites in the body that are prone to injuries at the enthesis. Notably these are the supraspinatus tendon in the rotator cuff of the shoulder and the anterior cruciate ligament (ACL) in the knee.

The rotator cuff is an arrangement of tendons that help stabilize the glenohumeral joint of the shoulder[9]. There are high numbers of injuries of the rotator cuff as people age. It has been estimated that 17 million people have rotator cuff tears and greater that 30% of the population over the age of 60 years have a rotator cuff tear of which 7-27% are full thickness tears and 13-37% are partial thickness tears[5,9,10]. To repair these injuries, approximately 75,000 surgeries are performed in the United States each year[5,10]. However, there is no gold standard for the treatment of rotator cuff tears. This is because of the complex anatomy of the shoulder and the relatively avascular tendons in the rotator cuff that do not lend to natural healing[9,10]. The most common method for repair is to secure the tendon to the humeral head with sutures and suture anchors, followed by extensive rehabilitation therapy[5,11]. However, these methods have a reported failure rates of 20-70%[9-12]. Even though the torn tendon is effectively replaced at its anatomic footprint, the functional interface is not regenerated[5]. It is the goal of rotator cuff repair is to restore the anatomic insertion of the tendon attachment which is the same goal for ligament repair.

The ACL is the most commonly injured ligament in the knee with an estimated 100,000 reconstructions per year in the United States and this number is steadily rising especially in the aging and the increasingly active younger populations[3,5,7]. Injury to the ACL causes instability of the knee and causes complications if not treated. Similar to the rotator cuff, the ACL is avascular and does not heal naturally[3,7]. For severe tears, primary reattachment is difficult so autografts or allografts are used. The most common graft is a bone-tendon-bone (BTB) graft taken from the patella and tibia in the knee of a cadaver or patient[5,13]. A bone tunnel is formed at the injured site between the femur and the tibia and the bone portion of the BTB is secured in the tunnel[13]. Another common technique is to harvest a hamstring tendon from cadaver or patient and secure it in the bone tunnels between the femur and tibia[5,13]. Successful repair can be achieved with these methods but also come with additional problems. Autografts are associated with additional patient surgeries, donor site morbidity, chronic joint pain, and osteoarthritis[3,5,7,14]. Allografts do not have these problems but do have limited availability, increased cost with sterilization, possible donor sourced pathogens, and decreased biological and mechanical properties through tissue processing[3,5,14]. The disadvantages of current graft methodologies reveal a clinical need to develop a graft that has the mechanical properties to transfer loads between tendon and bone while having the biologic capability to regenerate the anatomical interface needed for functional attachment. Biomaterial and cell based tissue engineering techniques have been used to address this problem[15]. In addition with the similarities between tendon and ligaments, with respect to anatomy, attachment site, and healing behaviors, a single technology developed for one could easily be modified for use with the other.

Current Research Strategies

Tissue engineering is the application of biomaterial scaffolds, cells, and signals to create a tissue *in vitro*[16]. Tissue engineering techniques are the primary method used in research to address enthesis repair and each component has an impact on what tissue is formed and how that tissue functions[13,17]. The purpose of the scaffold to act as a three-dimensional structure to allow cell attachment, cell migration, expression of cell signals, ECM deposition, and transfer of mechanical loads from surrounding tissues[6,18,19]. Ideally, this biomaterial matches the mechanical properties of the tissue being engineered and is degradable so that as the biomaterial scaffold is broken down, regenerated tissue is replaced. However, typically these two characteristic are inversely related with respect to mechanical properties[11]. Even so, commercially available synthetic materials used for tendon-to-bone repair include and non-degradable and degradable polymers. Non-degradable materials include polyester terepthalate (PET), polytetraflouroethylene (PTFE), and polypropylene (PP) and polycarbonate poly(urethanurea)[10,20-23] and degradable synthetic materials include poly(urethaneurea), and polylactic acid (PLA) [10,12,19]. These synthetic materials are attractive as scaffolds because material processing allows for control in 3-D structure and porosity which can have large impact on the tissue integration and mechanical properties of the repair. ECM is also a powerful signaler for tissue regeneration, so biologic ECM-based scaffolds have been considered[2,24]. Commercially available biologic ECM based materials include acellular dermal matrices (ACDM) from human, bovine, porcine, or equine sources[9-11,25]. These materials have shown rapid degradation and tissue integration but do not have the mechanical properties necessary to address functional loading. The scaffold needs to have tissue-specific

structural features for functional repair but also needs to be compatible with tissue-specific cell types.

Cells are important in tissue repair as they are responsible for matrix remodeling and tissue maintenance[4]. Most cell types have been differentiated to a specific function depending on the tissue. For tendon and ligaments, the primary cells are specialized fibroblasts, cartilage and fibrocartilage tissues contain chondrocytes, and bone has osteoblasts and osteoclasts. One strategy for cell selection in tissue engineering is to choose the fully differentiated cell type to deposit the ECM on the scaffold[26]. This is an attractive choice because these cell types tend to deposit mimetic ECM components seen in the natural tissue[26]. However, some specialized cells, such as tenocytes, have low metabolic activity, proliferate slowly, and are more suited for ECM maintenance rather than regeneration. Other fibroblast sources, such as dermal fibroblasts have been investigated for tendon and ligament repair[27]. Results showed that the dermal fibroblasts did produce ECM similar to the native ECM[27]. For bone tissue engineering typically only osteoblasts, bone forming cells are used in the absence of osteoclasts, bone resorbing cells. The other cell selection is an undifferentiated cell source. Specifically, for musculoskeletal tissues, mesenchymal stem cells (MSC) are used[6]. MSCs are adult stem cells that can differentiate into different cells types depending on the growth factors, cytokines, and ECM present[24]. MSCs are also metabolically active and deposit collagens readily[24]. However, MSCs need specific growth factors or chemical signals to fully differentiate into a specific cell type[6]. As of yet there are no established best cell type for each tissue. Many combinations of scaffold and cell type have the potential to show

tissue regeneration but depends on how the scaffold and cells signal the tissue to regenerate.

Extracellular matrix, growth factors, and mechanical stimuli are the signals that communicate to the body what to activate or deactivate in order to repair or regenerate the injured site[24]. Each cell type responds to specific combinations of signals from the extracellular environment to maintain or repair the tissue. Once these signals are identified they can be isolated, purified, and re-introduced into the tissue or cell environment, sometimes with dramatic effect[24]. For example, bone morphogenic protein-2 (BMP-2) is one growth factor that is commonly used for bone regeneration and when introduced into a muscle pouch is able to induce bone formation in the surrounding tissue. Similar responses with respect to tendon have been observed in tendon repair with the growth factor, BMP-12. Other growth factors are equally effective for their specific task[2]. In addition, mechanical stimuli can have a large impact on tissue response[2]. The classic example of how mechanical forces can affect tissues is Wolff's law in bone[28]. Essentially, bone will remodel according the forces acted upon the bone, so increases in cyclic forces will induce bone formation and decreases in stimulation will enhance bone resorption. There is also a similar response in tendon and soft tissues where tendon mass and ultimate strength increases with increased use and vise versa[2,29]. These techniques have been utilized by highly controlled mechanical strains systems to accurately control the application forces, the strain rates, the number of cycles, temperature, gas exchange, and remain sterile while in operation [2,11,30]. How these parameters are actually controlled is varied, but several researchers have taken on the challenge of creating these mechanical bioreactors to understand the role of mechanical stimulation in tissue

engineering[27,30-37]. These effects from the stimulation are most likely specific to each cell type and biomaterial scaffold combination used. Overall, tissue engineering is a complex and specific method to regenerate tissues. The complexity increases when multiple tissue types being engineered, such as the enthesis. With the right combination of scaffolds, cells, and signals, the body can be directed to regenerate the functional interface.

Hypothesis

The purpose of this research to explore a combination of biomaterial scaffolds, cell types, and ECM signals with tissue engineering techniques to aid in the repair of tendon-to-bone interfaces of both civilians and soldiers. We hypothesize that a commercially available scaffold can be modified with mechanically stimulated tissue specific ECM to induce faster tissue integration than the scaffold alone to aid in repair of the tendon-to-bone interface.

Specifically in this project, integration will be aided by modifying current commercially available scaffolds targeted for tendon repair with tissue-specific coating of cell deposited ECM. Distinct regions for tendon and bone will be formed on the scaffold using fibroblasts to deposit ECM to create a tendon region and osteoblasts to deposit ECM for the bone region. We then apply varying mechanically stimulation parameters to condition the cells while they deposit the ECM on the scaffolds. Chapter 2 focuses on the identification of the biomaterial scaffold from three commercially available materials. Chapter 3 describes the development of the co-culture protocol and characterization of co-cultured ECM coated scaffolds. Chapter 4 describes the methodology of applying mechanical forces to the cell seeded scaffold, characterizes ECM deposition on the scaffold and how that ECM activates tissue specific genes in MSCs.

CHAPTER 2: SCAFFOLD CONSIDERATIONS FOR TENDON/BONE INTERFACE ENGINEERING

INTRODUCTION

Tissue Engineering has become commonplace in biomedical research and regenerative medicine. Tissue engineering techniques have been established to create the paradigm consisting of combinations of scaffolds, cells, and signals[1]. Attempts to create various tissues *in vitro* have been reported by changing the scaffold's material, structural and mechanical properties, the cell types seeded, or the mechanical and chemical signals[2]. Often these reports have been focused on engineering single tissue types *in vitro* but recently a growing focus on the tissue engineering of multiple tissue types, or interfaces of tissues are being explored[3,4]. The targeted application has been on functional repair of interfaces of musculoskeletal tissues especially at the boundary between cartilage to bone, muscle to tendon, and tendon/ligaments to bone[3,5]. The work in this study focuses on the tendon/ligament to bone interface.

The tendon to bone interface, called the enthesis, transitions from a highly oriented non-calcified tension-based tissue to a calcified compression-based tissue in a very short distance[6-8]. The body achieves this transition naturally through a direct insertion[6]. Direct insertions accomplish attachment through a four layer transition from tendon to fibrocartilage to mineralized fibrocartilage to bone[7-10]. Examples of a direct insertion that are also sites of orthopedic intervention include the supraspinatus tendon of the shoulder rotator cuff and the anterior cruciate ligament in the knee[7,8]. The problem with these direct insertions for tendon to bone is that they are mostly avascular which

make natural repair difficult[7,11,12]. Tendon has specialized fibroblasts, called tenocytes, which have low metabolic activity and low healing capabilities and are used for maintenance of tendon extracellular matrix (ECM) and not necessarily tissue regeneration[11,13]. Since injuries at these interface sites do not heal well, surgery is often the best option for repair[6,7,11,12,14]. Grafts are necessary to regain mechanical function for very serious injuries[7]. Currently, autografts are considered the gold standard but have complications of their own including: extra harvesting surgeries, donor site morbidity, and increased risk of infection[12,13,15,16]. Allografts are also used clinically but are associated with possible immune rejection, problems with cellular infiltration, and incorporation into the surrounding tissues[12,13,15,16]. Synthetic grafts may provide an opportunity to engineer the mechanical properties to achieve fixation and include biologic components to aid in tissue integration.

In tissue engineering, the role of the synthetic grafts is as a biomaterial scaffold to act as a three-dimensional structure to allow cell attachment, cell migration, expression of cell signals, extracellular matrix (ECM) deposition and transfer of mechanical loads from surrounding tissues[13,17,18]. There have been different scaffolding materials that have been tested *in vitro* and *in vivo* to improve tendon to bone fixation. Commercially available materials that have been used for tendon to bone repair include various braids, wovens, and knits of non-degradable polyester terepthalate (PET), polytetraflouroethylene (PTFE), and polypropylene (PP) and polycarbonate poly(urethaneurea)[19-23]. Degradable synthetic materials that have been used include poly(urethaneurea), and polylactic acid (PLA) [18,23,24]. Commercially available biologic ECM based materials include acellular dermal matrices from human, bovine, porcine, or equine sources[23,25,26]. These devices

have been approved by the FDA because they are single biomaterials or, in the case with dermal matrices, labeled as tissues[26]. Other devices which are gaining interest are combination devices of a biomaterial with growth factors or biologic factors including cells. These combination technologies could take up to a decade or more to gain regulatory approval. There may be an opportunity to expedite therapeutic technology through the FDA by modifying a commercially available graft with decellularized ECM coatings to accommodate the mechanical and biologic needs of the tendon-to-bone interface.

Specifically in regards to this study, integration will be aided by modifying commercially available scaffolds targeted for tendon repair with a tissue specific coating of cell deposited ECM. Fibroblasts will be used to deposit ECM to create a tendon region and osteoblasts will be used to deposit ECM for the bone region. This study focuses on single culture of both fibroblasts and osteoblasts to evaluate a non-degradable, degradable, and biologic substrates as candidates for a tendon to bone interface scaffold. After 28 days in culture, the scaffolds will be evaluated quantitatively and qualitatively for mechanical properties, cell survival, and ECM deposition.

METHODS

Materials

Representative commercially available degradable, non-degradable, and biologic scaffolds were selected for testing. Fabrics were also targeted due to the high surface area and tensile strength inherent in the fabric structure. The non-degradable custom fabric scaffold is polyethylene terephthalate (PET) [Biomedical structures, Warwick, RI] and has been previously used in research in our laboratory. The degradable fabric is X-

Repair®, a commercially available polylactic acid (PLA) woven fabric provided by Synthasome Inc, CA. X-Repair® is currently used for surgical reinforcement for tendon rotator cuff repair. The biologic representative is BioTape® (BT), an acellular porcine collagen dermal matrix provided by Wright Medical Technology, TN. BioTape® is currently used for reinforcement of tendons at suture sites after repair.

The BioTape samples come sealed in sterile packaging, so additional cleaning and sterilization were not necessary. Care was taken to keep the BioTape sterile using aseptic technique while preparing the samples for cell culture. The fabric scaffolds were not provided in sterile condition so cleaning and sterilization was necessary. Fabric samples were cut to the appropriate size based on the experiment to be performed. The edges were fused thermally to prevent unraveling of the fabric. The fabrics were sonicated in an ultrasonic bath in a 1% by volume triton-x 100 detergent solution to remove any possible oils or dirt that may be present after manufacturing. The samples were well rinsed several times in deionized water to remove any residual detergent. The fabric samples were further soaked in 70% ethanol (EtOH) and placed under UV light for 1 hour, flipped, and repeated for another hour to sterilize the scaffolds. Samples undergoing mechanical testing were not sterilized.

Mechanical Testing

Prior to cell culture, the scaffolds were evaluated for basic mechanical properties and their potential load bearing capabilities. Each scaffold type (n=5) was cut to 12.5 mm width and 50 mm length. All samples were fully hydrated in phosphate buffered saline (PBS) before loading. Scaffolds were clamped into an Instron 33R-4465 load frame (Instron, Norwood, MA) and loaded in tension at a rate of 25mm/min until failure.

Measurements were taken using a 500 N load cell at a sample rate of 100 Hz using Bluehill 2 software. The PET and PLA fabrics average fiber diameter was measured under microscopy to calculate cross sectional area. BioTape was measured directly with digital calipers (Mitutoyo, Aurora, IL). The stress strain curve was calculated for each test specimen. The elastic modulus, ultimate strength, and strain at failure was taken from the stress strain curve and averaged for each scaffold type.

Cell Seeding and Culture

After sterilization, scaffolds were soaked in α-MEM (Hyclone, Waltham, MA) containing 10% fetal bovine serum (FBS) (Hyclone, Waltham, MA) for 1 hour prior to cell seeding. Scaffolds and tissue culture plastic (TCP) controls were seeded with NIH 3T3 mouse fibroblasts (FB) (CRL-1658 ATCC, Manassas, VA) or MC 3T3-E1 mouse calvarial osteoblasts (OB) (CRL-2593 ATCC, Manassas, VA) in single culture. The scaffolds were seeded at a density of $1x10^5$ cells/mm^2 in 24 well plates. Cells were allowed to proliferate for 5 days to allow cells to migrate over the fabric and BioTape. Day 5 is considered time zero, then samples were analyzed at days 1, 7, 14, 21, 28 afterwards. At each time point, each scaffold group type had an n=4. All seeded scaffolds were grown in α-MEM containing 10% FBS + 1000 U/mL penicillin, 1000 μg/mL streptomycin, 2.5 μg/mL amphotericin-B (Gibco, Grand Island, NY). At every medium change, ascorbic acid was freshly added to a concentration of 25 μg/mL.

SEM Imaging and Live/Dead Staining

The scaffolds were characterized using scanning electron microscopy (SEM). Each scaffold type was imaged with and without cell seeding. Scaffolds were also imaged for cell viability over the course of cell culture. Both fabric types and TCP were

imaged using Live/Dead fluorescent stain (Invitrogen, Grand Island, NY) at days 1, 7, 14, 21, and 28 for each cell type.

Matrix Digestion

At each time point, samples were removed from the 24 well plate and placed in a 2 mL microcentrifuge tube. Then 1 mL of a buffered enzymatic digestion solution of 100 μg/mL proteinase-K (Promega, Madison, WI) was added to each sample. All samples were then placed in an oven at 60°C overnight. The following day phenylmethanesulfonylfluoride was added to a final concentration of 5mM to inhibit proteinase-K. All samples were homogenized using a sonic dismembrator (Fisher Scientific, Waltham, MA) and aliquots were taken from each sample to perform DNA, GAG, and hydroxyproline (HYP) assays. Volumes were carefully recorded and monitored for normalization during analysis.

DNA Analysis (Pico Green Assay)

DNA was analyzed using a picogreen assay (Invitrogen, Grand Island, NY) which tests for double stranded DNA and was used as a normalization parameter for the other matrix components. Aliquots of 20 μL were used and the assay was performed according to the manufacturer's instructions.

Glycosaminoglycan (GAG) Analysis (Alcian Blue)

GAG content was quantified using an alcian blue (National Diagnostics, Atlanta, GA) precipitation reaction [16,27,28]. This assay takes advantage of the precipitates formed from the binding of alcian blue to sulfated GAGs. The precipitates are centrifuged and rinsed, then dispersed to read with a spectrophotometer. Briefly, 300 μL aliquots of every sample and the chondroitin sulfate standards were incubated for 2 hours with 500

μL of 25mM buffered alcian blue solution. Samples were centrifuged for 5 minutes at 16,000xg to form a pellet and aspirated. Pellets were then rinsed with 40% EtOH/buffer solution and recentrifuged for 5 minutes at 16,000xg. The supernatants were aspirated and 500 μL of 10% SDS in water was added to resuspend the pellet. Samples were resuspended using the sonic dismembrator. The resuspended solutions were transferred to a 96 well plate and read on a spectrophotometer (Molecular Devices, Sunnyvale, CA) at a wavelength of 620 nm.

Collagen Analysis (Hydroxyproline assay)

Collagen content was quantified by direct measurement of the amino acid, hydroxyproline [29,30]. Collagen proteins are hydrolyzed to amino acids using 6M HCl, amino acids are oxidized to a pyrrole with chloramine-T, and a chromophore is formed using Ehrlich's reagent. Briefly, aliquots were taken from each sample and the volumes were recorded. The aliquots were mixed with 1 mL 6M HCl and placed in an oven at 100°C overnight. The solutions were then transferred to 25 mL Wheaton vials and 5 mL deionized (DI) water was added. Samples were frozen, lyophilized, re-hydrated with 5 mL DI water, frozen and lyophilized a second time to remove the acid. Samples were rehydrated in 1 mL DI water and aliquots were reacted with chloramine-T solution for 20 minutes at room temperature. Then Ehrlich's reagent, 4-(dimethylamino) benzaldehyde dissolved in 2:1 n-propanol: perchloric acid, was added to each sample and reacted for 20 minutes at 60°C to induce a colorimetric response. Absorbance was measured at a wavelength of 550 nm.

BioTape Considerations

The third scaffold type is BioTape and it has been segregated from the other scaffolds simply because its characterization and response in cell culture was much different than the other scaffolds. The first difference encountered with BioTape is that the major determinant we used to evaluate a successful scaffold is deposition of extracellular matrix onto the scaffolds surface. BioTape is already comprised of a dense network of dermal matrix which consists of collagen and GAGs plus many other matrix proteins[26]. Control standard samples (n=12) were dried thoroughly, weighed, and kept in sterile PBS for the duration of the 4 week study without cell seeding. After the study, these standards were assayed for DNA, GAG, and HYP. These amounts were then averaged and used to subtract the baseline ECM content from the BioTape samples to determine the amount of newly deposited ECM.

Statistics

The data for each test were collected and averaged. BioTape was normalized to its pre-study weight. The non-cultured BioTape controls were used to subtract the ECM contribution from the BioTape away from the ECM deposited by the cells. Both the GAG and HYP data for each scaffold was normalized to DNA and error was propagated due to normalization. One-way ANOVA with Student-Newman-Kuels (SNK) post- hoc tests were performed on the mechanical testing and BioTape data, and all other data were analyzed using a two-way ANOVA with SNK post-hoc test.

RESULTS

Mechanical Testing

Table 1 shows the mechanical performance of each hydrated scaffold type. All groups are significantly different from each other in maximum load, elastic modulus, ultimate strength, and strain at failure. Compared to the other scaffolds, the non-degradable PET fabric has the highest elastic modulus at nearly 2 GPa and ultimate strength of 326 MPa but also has the lowest load until failure at 78 N due to the smallest amount of material contributing to loading. The degradable PLA scaffold has a larger cross-sectional area than the PET and accommodated the highest loads of the three scaffolds tested. The PLA also had an elastic modulus of 1.35 GPa and an ultimate tensile strength of 301 MPa, significantly less than the PET. The hydrated biologic BioTape scaffold had the highest cross-sectional area of the scaffolds and at 144 N, accommodated almost double the loading of the PET scaffold. However, once calculated, the elastic modulus of the BioTape was two orders of magnitude lower than the other scaffolds at 38 MPa and the ultimate tensile strength was an order of magnitude lower at 12 MPa. The strain at failure of the non-degradable PET was significantly lower than the degradable PLA at and the BioTape scaffolds.

TABLE I. Tensile testing of each scaffold type.

Scaffold	Maximum Load (N)	Cross sectional Area (mm^2)	Elastic Modulus (MPa)	Ultimate Strength (MPa)	Strain at Failure (%)
PET	78.3 ± 4.3*	0.24	2055 ± 118*	326 ± 18*	25 ± 3*
PLA	240.6 ± 17.7*	0.80	1353 ± 26*	301 ± 22*	38 ± 34
BT	144.7 ± 18.2*	12.25	38 ± 7*	12 ± 2*	40 ± 3

Data are presented as means ± standard deviations. *Within columns, groups are statistically different from the other groups, $p < 0.01$. PET = polyester fabric, PLA = polylactic acid fabric, BT = BioTape acellular porcine matrix. Statistics were not performed on cross sectional area.

SEM

Scanning electron microscopy was performed to show topographical differences between scaffold types. Each cell seeded scaffold is presented in Figure 1, with ECM deposition early in the growth study. All scaffolds supported cells and matrix deposition was noted on all scaffolds after culture at 4 days. The surfaces of the fibers in both fabrics are smooth with little surface roughness. This morphology did not hinder cell attachment or ECM deposition. The BioTape was more difficult to assess new ECM deposition, as it is already ECM based, however at higher magnification seeded cells were observed. Figure 1 shows comparisons of seeded and non-seeded PLA scaffolds (A & D). Image E shows a cell sheet that became detached from the underlying PET fabric during the dehydration and coating step. Images C and F show BioTape with cells at 100x magnification (C) and with no cell seeding at 75 x magnification (F). The surface appears to have a smoother surface after cell seeding.

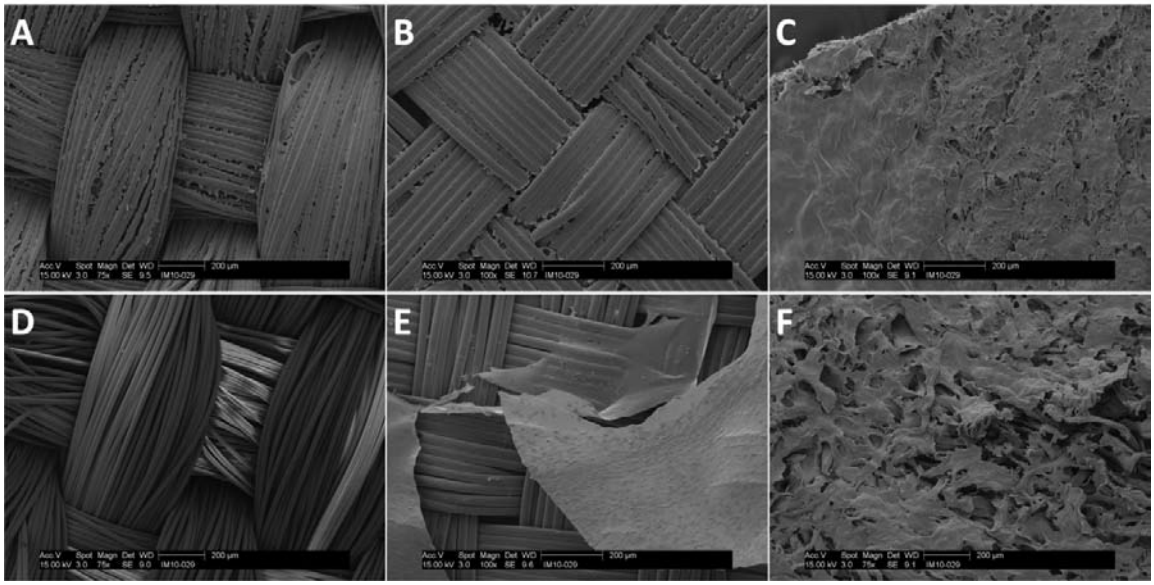

FIGURE 1. SEM images of three scaffold types at 4 days. Early ECM deposition is visible on each seeded scaffold. (A) PLA Fabric with cells – 75x magnification, (B) PET Fabric with cells – 100x magnification, (C) BioTape with cells – 100x magnification, (D) PLA fabric without cells – 75x magnification, (E) PET fabric with a detached cell sheet exposing the fabric underneath – 100x magnification, (F) BioTape without cells – 75x magnification.

Live Dead Staining

Images from Live/Dead imaging of the cells seeded on substrates are shown in Figure 2. Cells proliferated and deposited matrix on the scaffolds over the course of 28 days. At each subsequent seven-day time point, the images appeared to become increasingly blurry. It is hypothesized the lack of focus is due to continuous ECM deposition that diffuses the light. It is also difficult to acquire a high magnification image of the cells on fibers because none of the scaffolds provide a flat surface. The fabrics have multiple focal planes between the interweaving fibers. As seen in Figure 3, once a focal plane is selected the fibers are translucent which further diffuses the fluorescence of

the cells. Even though the fibers seem to autofluoresce, they do not. Therefore, the best qualitative data were observed from 4x magnification images. Cells proliferated and viability remained high for the length of the study.

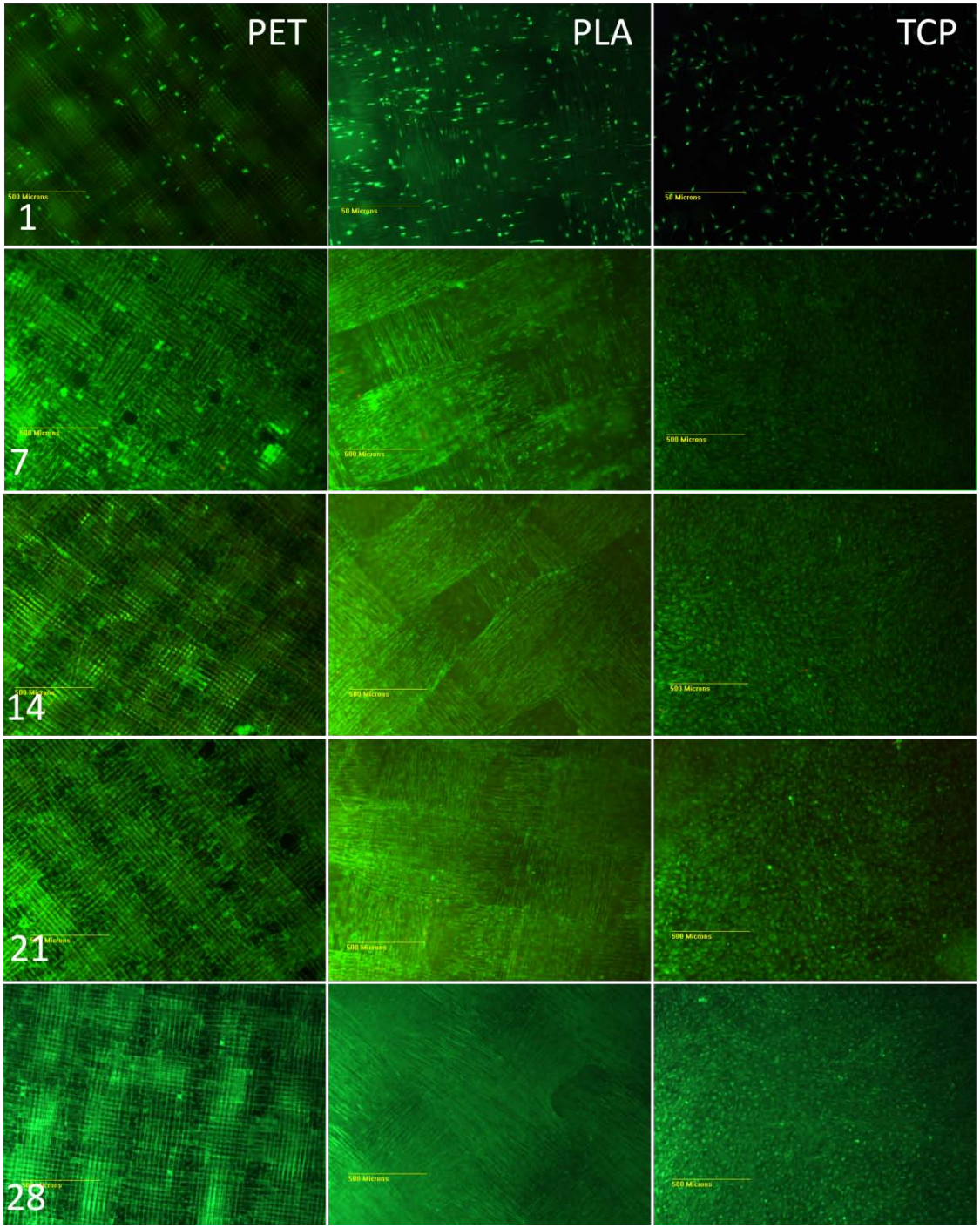

FIGURE 2. Series of Live/Dead Images on TCP, PET, PLA with FB. Images were recorded over the 28 day study. All magnifications are 4x. Scale bar in every image is 500 microns. Cells were seeded at $1x10^5$ cells/mm^2. Cells proliferated until confluence. Cell viability remained high over the course of the study.

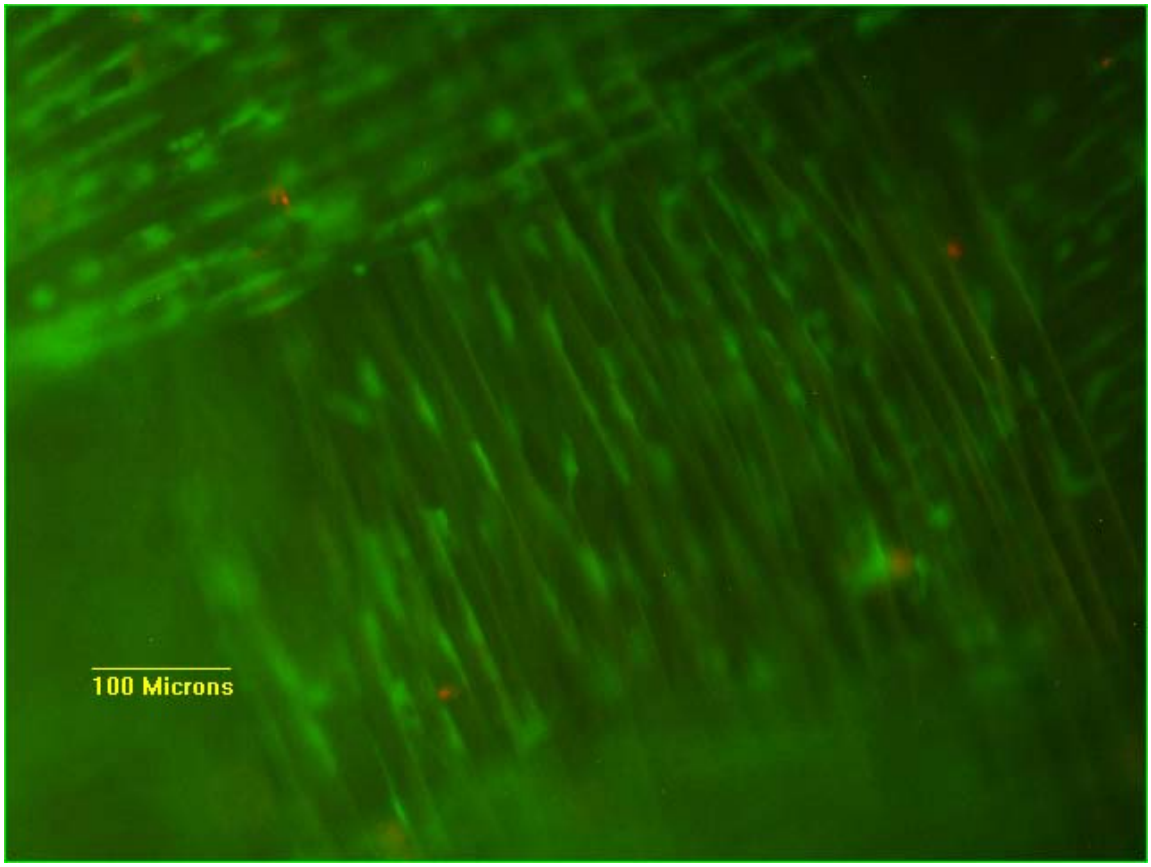

FIGURE 3. Live Dead image of FB on PLA fabric at Day 7 - 10x magnification. This image demonstrates the multiple focal planes due to the fabric surface as well as the fluorescence of the cells observed through the translucent fibers. The vast majority of cells were live (green) while few dead cells (red) were observed.

DNA (Picogreen assay)

The DNA data used for normalization are presented in Figure 4. Both fabric types supported cells but not to the level of the tissue culture plastic control. DNA was present on both scaffolds and TCP over the entire 28 day study. Only the FB had significantly higher DNA values for the PLA over the PET scaffold for days 7, 14, and 28. There were approximately equal amounts of DNA regardless of cell type indicating the scaffolds were equally supportive of the cells.

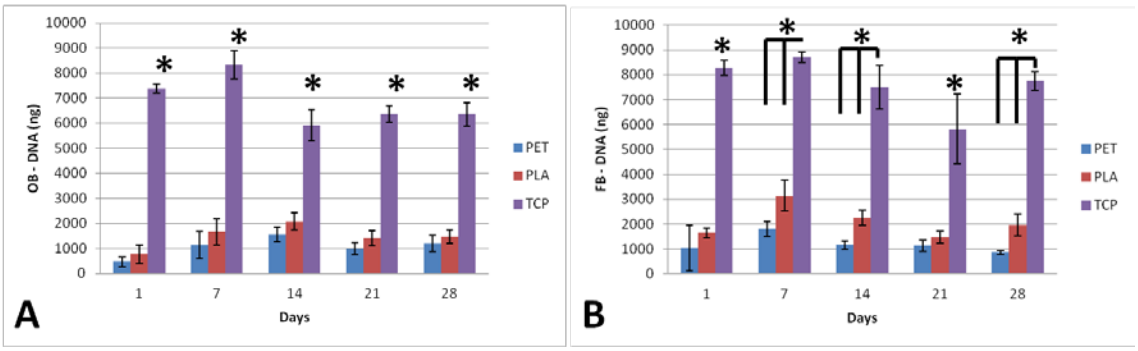

FIGURE 4. DNA data [means ± standard deviations] from OB (A) and FB (B) cultured on PLA and PET scaffolds and a TCP control (BioTape is presented separately). With respect to the OB, the TCP control was significantly greater than the scaffolds. There was no difference in scaffolds. For the FB, The TCP was also significantly greater than the scaffolds. On days 7, 14, and 28 the PLA scaffold had significantly more DNA than the PET scaffold. *$p<0.05$.

GAG (alcian blue assay)

Using the alcian blue method, deposited GAG amounts were quantified and normalized to DNA. Figure 5 shows that both scaffold types promoted significantly more GAG/DNA than the TCP control for both cell types at most time points. There was no significant difference between PLA and PET scaffolds for OB. On day 1 PLA fabric had significantly more GAG/DNA than the PET scaffolds, however by day 28 PET had significantly more deposition per cell. Day 1 was observed to have a high GAG per cell amount when compared with the other time points. This is most likely due to the lower DNA amounts on the scaffolds at day 1, so that any GAG present will be amplified. For the remaining time points, GAG per cell tended to remain constant for the osteoblasts or increase slightly for the fibroblasts.

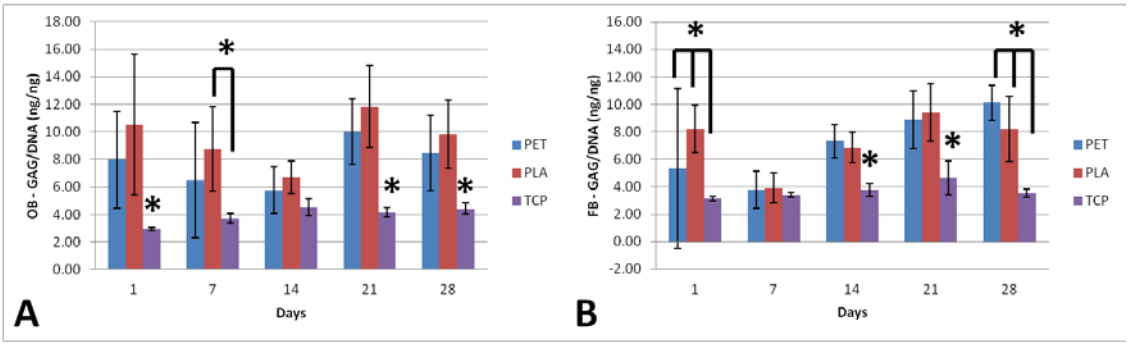

FIGURE 5. GAG data [means ± standard deviations] normalized to DNA for PLA and PET scaffolds and a TCP control for both OB (A) and FB (B). Both scaffolds had significantly more GAG/ DNA than the TCP control for most time points. There was no significant difference between PLA and PET scaffolds for the OB. PLA supported significantly more GAG/DNA than the PET scaffold on days 1 but the PET scaffold had higher amounts on day 28 for the FB. *$p<0.05$.

Hydroxyproline Content

Collagen content of deposited ECM was measured using the hydroxyproline assay. Figure 6 shows normalized HYP/DNA amounts for each type on the scaffolds (BioTape is presented separately). For the osteoblasts, with exception of the PET scaffold on day 1, there was no significant difference of HYP/DNA for any of the other scaffolds on any time point. With respect to the fibroblasts, the PET scaffold did support significantly more HYP/DNA than the PLA scaffold or TCP control. As seen previously with the GAG/DNA data, day 1 was observed to have a high HYP/DNA amount due to the lower initial cell numbers on the scaffolds making any deposited hydroxyproline seem higher. For the remaining time points, HYP/DNA tended to slightly increase especially for fibroblasts on the PET scaffolds.

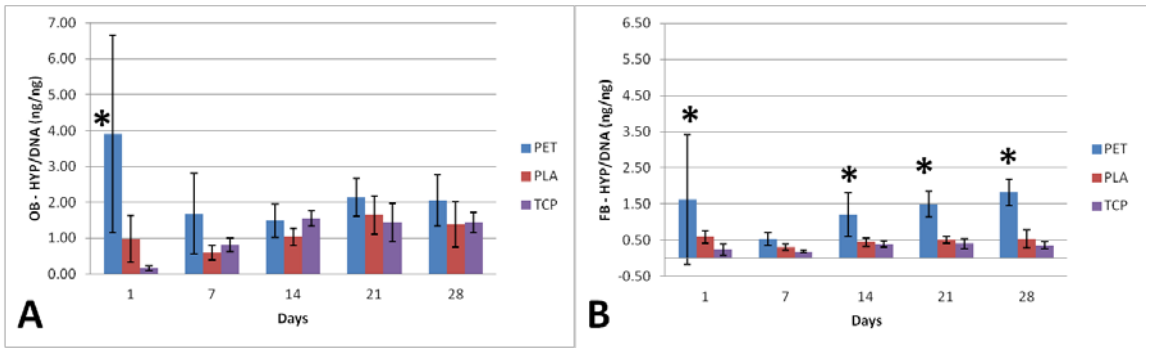

FIGURE 6 – Hydroxyproline data [means ± standard deviations] normalized to DNA for PLA and PET scaffolds and a TCP control for both OB (A) and FB (B). For the OB, the PET fabric had significantly higher collagen content per cell on Day 1. For the FB, the PET fabric had significantly higher collagen per cell on day 1, 14, 21 and 28. There was no difference between the PLA scaffold and TCP control. *$p<0.05$.

BioTape

As mentioned previously, BioTape is an ECM based biologic scaffold comprised of the same ECM components assayed for in this study. Therefore, all data presented in Figure 7 have been normalized to the 12 standard samples without cell seeding in order to subtract out the baseline BioTape signal. The signal measured from the BioTape standards was much higher than the signal detected from the samples with cell deposited ECM. Another complication with normalizing to non-seeded acellular BioTape standards was that large amounts of DNA were extracted from the BioTape. This suggests that the DNA is not completely removed from the BioTape matrix[25,26] which further complicates DNA normalization for the GAG and collagen assays. Once normalized to the BioTape standards, most of the data was near zero or negative. DNA measurements of seeded scaffolds increased over the course of the study for both cell types indicating cell proliferation after seeding. Both GAG and HYP amounts measured decreased over the duration of the study. Once normalized to DNA and the BioTape

baseline, the GAG and HYP amounts had steadily decreasing values. There was a significant difference from day 1 to days 21 and 28 for the GAG/DNA for both cell types. There was no significant change in HYP/DNA for either cell type over the 28 days.

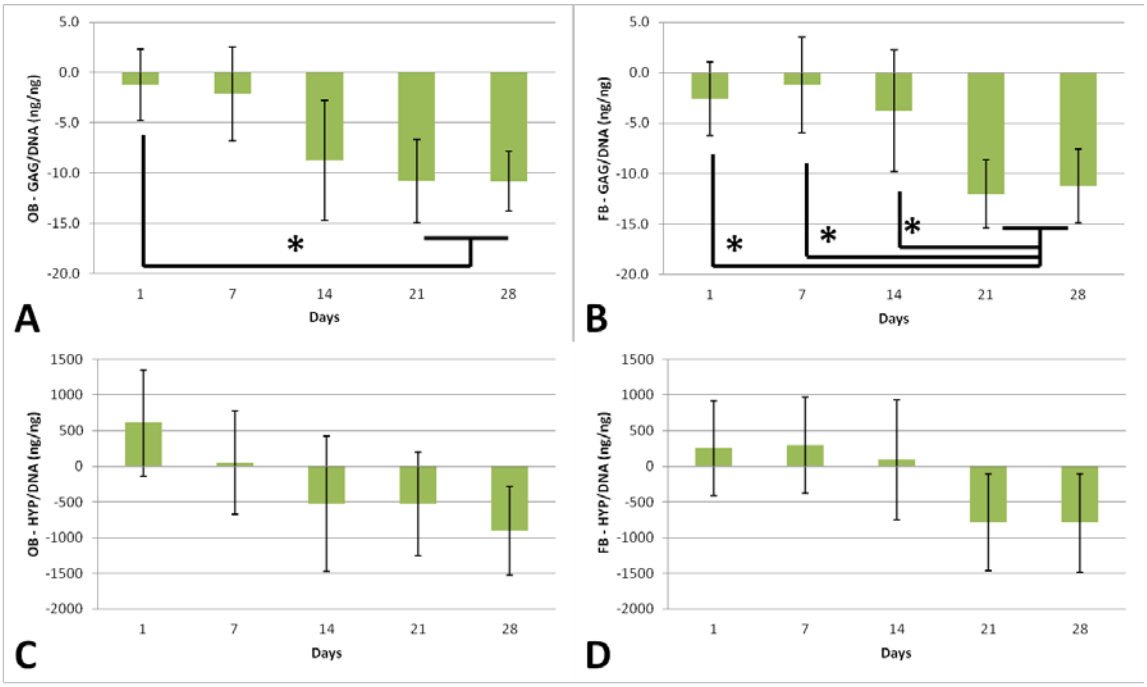

FIGURE 7 – Both normalized GAG and HYP data [means ± standard deviations] for the BioTape scaffolds. (A) GAG/DNA for OB. There was a significant decrease from day 1 to days 21 and 28. (B) GAG/DNA for FB. There was no difference between days 1, 7 and 14. However, there was a significant decrease with days 21 and 28. (C) HYP/DNA for OB. There was not a significant decrease in HYP/DNA. (D) HYP/DNA for FB. There was no significant decrease in HYP/DNA. *$p<0.05$.

DISCUSSION

The purpose of this study was to determine an appropriate biomaterial scaffold for tissue engineering of the tendon to bone interface for future evaluations. The scaffold options were commercially available candidates chosen to compare characteristics of a

non-degradable, degradable and a biologic biomaterial. The overall function of tissue engineering scaffolds is to allow cell attachment, cell migration, expression of cell signals, extracellular matrix (ECM) deposition and transfer of mechanical loads from surrounding tissues[5,31]. As biomaterials, all three scaffolds allowed for cell attachment, proliferation and had good cell viability with fibroblasts and osteoblasts based on SEM and Live/Dead imaging. For use in tendon to bone interfaces, the scaffolds need to combine the properties of tendon and bone tissue-engineering scaffolds into a single construct. This means balancing mechanical properties and biologic responses of the scaffold. The main cause of graft failure is insufficient functional integration with the surrounding tissue to achieve mechanical stability at the interface[16]. In the past, PET scaffolds were used in ligament repair with limited success[20-22]. Scaffolds showed good initial fixation and results but long-term the implants loosened at the surgical site and did not provide stability. PET was included in this study because modifying the non-degradable with a biologic coating may help bridge the mechanical benefits of synthetic biomaterials biologic with the benefits of ECM based biomaterials.

The representative ECM components selected to determine cell based ECM deposition on the scaffolds were glycosaminoglycans and collagen. GAGs are important matrix components for stabilizing ECM and collagen fibrils in connective tissues, bind water to create hydrostatic pressure, and show general matrix deposition[32]. Chondroitin sulfate is the most prevalent GAG in bone and is also present in tendon. GAGs participate in other tendon important proteoglycans, such as decorin and biglycan, which act as crosslinkers for collagen aiding in an increase of tensile strength [33]. The assay we performed, alcian blue, is used in a precipitation reaction with sulfated GAGs to allow for

quantification [27,28]. This reaction binds to all sulfated GAGs, but not to non-sulfated GAGs. For the purposes of this study it was not necessary to determine the specificity of individual GAGs, since sulfated GAGs are present in both bone and tendon ECM[32]. In our studies, once the GAG data were normalized to DNA, both of the fabric scaffolds had higher GAG deposition per cell compared to the TCP control. This may be due to the 3-D nature of the scaffolds that has higher surface area for the cells, rather than forming a monolayer sheet on the TCP. Both cell types deposited significantly more GAG on the PET and PLA scaffolds compared to TCP control. We also found that after the initial GAG deposition on the scaffolds, the OB deposited GAG per cell leveled off while the FB deposited GAG per cell increased over the study. A study by Visser et al. using the same PLA fabric with primary tenocytes showed that total sulfated GAG amount remained unchanged with time[18].

The other ECM component measured was collagen. It is the major component found in connective tissues, especially bone and tendon [3,10,33]. Hydroxyproline comprises 10.8% of the amino acids in collagen[29,30] and is relatively specific to collagen. However, this assay does not distinguish between collagen sub types, such as collagen I, II, and III, all of which are found in different parts of the enthesis. Also while hydroxyproline is mostly seen in collagens, it is also 1% of the amino acids found in elastin, another matrix component in tendon[13]. Elastin exists as less than 3% of the ECM content in tendon[3] so it was not a concern for measuring potential small amounts of elastin-contributing hydroxyproline along with the major contributing collagen based hydroxyproline. There were not as many differences between scaffolds for collagen deposition. The fibroblasts did deposit significantly more collagen per cell on the PET fabric than the other

scaffolds. It is possible, there may have been some acidic by products[34] or small amounts of degradation of the PLA over the 4 week study causing less accumulated amounts of collagen compared to the non-degradable PET fabric[13]. Further testing is needed to confirm this hypothesis. A continuous deposition of collagen on the PLA fabric over 28 days was also reported by Visser, et al[18]. Hydroxyproline is a good first step and selection assay for the differing scaffold types. In future studies, more specific collagen subtypes can be studied to distinguish between tendon, bone, and the fibrocartilage transition zone.

ECM accommodation is just one factor in the scaffold selection criteria. Mechanical stability is another major factor in whether a scaffold can be a successful graft. The primary cause of graft failure occurs because of mechanical stability at the interface junction and lack of functional intergration[16]. This is one reason why synthetic grafts have been so attractive as scaffolds because the mechanical properties can be tailored to suit the needs of the tissue being engineered [12]. The mechanical strength of the scaffolds was measured through tensile testing, since tendons are primarily under tensile loads. Depending on which tendon is tested and which methods of testing are used, tendon can have a range of mechanical values. The elastic modulus of tendon typically ranges between 500-1850 MPa, strains at failure are between 50-125 MPa, and failure strains are 13-32% for bone-tendon-bone specimens or 5-16% for tendon proper[35]. The PET scaffold in comparison has an elastic modulus and ultimate strength that are greater than native tendon and a failure strain within the range of a bone-tendon specimen. Similarly, the PLA scaffold has an elastic modulus that falls within the range of native tendon and a higher ultimate tensile strength and higher strain at failure than

tendon. It is promising that if a suitable fixation method could be attained then the mechanical properties of the scaffolds could accommodate loading until tissue integration is achieved. The biologic scaffold had a mechanical performance significantly lower than the other tested scaffolds. Biologic based scaffolds, such as acellular dermal grafts and small intestine submucosa, have not been able to establish mechanical properties equal to native tissues, and typically have more than an order of magnitude less than tendon[25,26]. Our mechanical testing concurred with these previous findings. It should be noted that, as a commercial product, these products, including BioTape, are not designed nor indicated for direct loading of tendon, but rather as an augmented wrap around tendon sutures to reinforce healing[25,26,36]. The aim of this project, however, is to select a scaffold that can assist in transferring some of the mechanical loading after repair during healing.

BioTape also had several other *in vitro* complications associated with analyzing the newly deposited or cell mediated ECM because of the high amounts of the baseline BioTape ECM. Another complication is the residual DNA found in the BioTape standards which complicates normalization of the ECM components. Other researchers have found that ECM based materials have varying successes of removing cells, cell components, and DNA from the ECM [13,25,26]. The third unexpected result is that over the course of the 28 day study, with no noticeable breakdown of the BioTape, the ECM components that were quantified in the BioTape decreased. It is possible that the cells could begin a remodeling type behavior by excreting MMPs in the form of collagenases to breakdown the matrix or to migrate through the tissue[37-39], but further evaluations would need to be performed to confirm this hypothesis. While studies using BioTape

have reported good *in vivo* performance[25,26], its effectiveness as an *in vitro* tendon to bone scaffold was obscured because of the negative measured ECM values, and high ECM baseline signal compared to the newly cell deposited ECM. There is also a high amount of residual DNA that obscures cell quantification and normalization.

In conclusion, although BioTape is reported to perform well in clinical studies, the scaffold was difficult to assay *in vitro* and did not demonstrate the mechanical strength necessary as a directly loaded tendon scaffold. While the PET and the PLA had significantly higher ultimate strengths than the BioTape, the PLA fabric has a modulus within the range of reported tendon values. FB did deposit more collagen on the PET scaffolds but based on the other cellular depositions of ECM both fabric scaffolds performed very similarly. Degradable scaffolds do have the added advantage that allow for replacement with host tissue as the scaffold degrades. The non-degradable scaffold does not have that opportunity and will be implanted for the life of the patient. With mechanical performance and the ECM deposition being similar between both scaffold types, for our application, the degradable PLA fabric scaffold is the most appropriate scaffold for the tendon to bone interface and future studies will expand using this scaffold. Future studies include a more efficient cell seeding technique for scaffolds, analyzing ECM deposition using more specific ECM components, and co-culture of fibroblasts and osteoblasts on a single scaffold to create a more mimetic tendon-to-bone scaffold.

FUNDING

This project was funded by the DOD PRORP- USAMRMC W81XWH-10-1-0768 grant and by the Biomaterials Applications of Memphis (BAM) Laboratories in the Biomedical Engineering Department at the University of Memphis.

REFERENCES

1. Langer R, Vacanti JP. Tissue engineering. Science 1993;260(5110):920-6.

2. Lu HH, Subramony SD, Boushell MK, Zhang X. Tissue engineering strategies for the regeneration of orthopedic interfaces. Ann Biomed Eng 2010;38(6):2142-54.

3. Yang PJ, Temenoff JS. Engineering orthopedic tissue interfaces. Tissue Eng Part B Rev 2009;15(2):127-41.

4. Lu HH, Jiang J. Interface tissue engineering and the formulation of multiple-tissue systems. Adv Biochem Eng Biotechnol 2006;102:91-111.

5. Moffat KL, Wang IN, Rodeo SA, Lu HH. Orthopedic interface tissue engineering for the biological fixation of soft tissue grafts. Clin Sports Med 2009;28(1):157-76.

6. Hashimoto Y, Yoshida G, Toyoda H, Takaoka K. Generation of tendon-to-bone interface "enthesis" with use of recombinant BMP-2 in a rabbit model. J Orthop Res 2007;25(11):1415-24.

7. Zhang X, Bogdanowicz D, Erisken C, Lee NM, Lu HH. Biomimetic scaffold design for functional and integrative tendon repair. J Shoulder Elbow Surg;21(2):266-77.

8. Benjamin M, Milz S, Bydder GM. Magnetic resonance imaging of entheses. Part 1. Clin Radiol 2008;63(6):691-703.

9. Wang IE, Shan J, Choi R, Oh S, Kepler CK, Chen FH, Lu HH. Role of osteoblast-fibroblast interactions in the formation of the ligament-to-bone interface. J Orthop Res 2007;25(12):1609-20.

10. Dourte LM, Kuntz AF, Soslowsky LJ. Twenty-five years of tendon and ligament research. J Orthop Res 2008;26(10):1297-305.

11. Abousleiman RI, Reyes Y, McFetridge P, Sikavitsas V. Tendon tissue engineering using cell-seeded umbilical veins cultured in a mechanical stimulator. Tissue Eng Part A 2009;15(4):787-95.

12. Cooper JA, Lu HH, Ko FK, Freeman JW, Laurencin CT. Fiber-based tissue-engineered scaffold for ligament replacement: design considerations and in vitro evaluation. Biomaterials 2005;26(13):1523-32.

13. Kuo CK, Marturano JE, Tuan RS. Novel strategies in tendon and ligament tissue engineering: Advanced biomaterials and regeneration motifs. Sports Med Arthrosc Rehabil Ther Technol;2:20.

14. Joshi SD, Webb K. Variation of cyclic strain parameters regulates development of elastic modulus in fibroblast/substrate constructs. J Orthop Res 2008;26(8):1105-13.

15. Soon MY, Hassan A, Hui JH, Goh JC, Lee EH. An analysis of soft tissue allograft anterior cruciate ligament reconstruction in a rabbit model: a short-term study of the use of mesenchymal stem cells to enhance tendon osteointegration. Am J Sports Med 2007;35(6):962-71.

16. Spalazzi JP, Dagher E, Doty SB, Guo XE, Rodeo SA, Lu HH. In vivo evaluation of a multiphased scaffold designed for orthopaedic interface tissue engineering and soft tissue-to-bone integration. J Biomed Mater Res A 2008;86(1):1-12.

17. Yang B, Zhang Y, Zhou L, Sun Z, Zheng J, Chen Y, Dai Y. Development of a porcine bladder acellular matrix with well-preserved extracellular bioactive factors for tissue engineering. Tissue Eng Part C Methods;16(5):1201-11.

18. Visser LC, Arnoczky SP, Caballero O, Kern A, Ratcliffe A, Gardner KL. Growth factor-rich plasma increases tendon cell proliferation and matrix synthesis on a synthetic scaffold: an in vitro study. Tissue Eng Part A 2010;16(3):1021-9.

19. Guidoin MF, Marois Y, Bejui J, Poddevin N, King MW, Guidoin R. Analysis of retrieved polymer fiber based replacements for the ACL. Biomaterials 2000;21(23):2461-2474.

20. Seitz H, Marlovits S, Schwendenwein I, Muller E, Vecsei V. Biocompatibility of polyethylene terephthalate (Trevira (R) hochfest) augmentation device in repair of the anterior cruciate ligament. Biomaterials 1998;19(1-3):189-196.

21. Jenny JY, Jenny G, Daubresse F. Replacement of the Anterior Cruciate Ligament with Three Different Dacron Prostheses. International Orthopaedics 1991;15(1):23-28.

22. Seitz H, Lang S, Marlovits S, Mousavi M, Kolonja A. Repair of the anterior cruciate ligament - a morphological study in sheep. Medizinische Welt 1998;49(12):610-617.

23. Ricchetti ET, Aurora A, Iannotti JP, Derwin KA. Scaffold devices for rotator cuff repair. Journal of Shoulder and Elbow Surgery 2012;21(2):251-265.

24. Derwin KA, Codsi MJ, Milks RA, Baker AR, McCarron JA, Iannotti JP. Rotator cuff repair augmentation in a canine model with use of a woven poly-L-lactide device. J Bone Joint Surg Am 2009;91(5):1159-71.

25. Aurora A, McCarron J, Iannotti JP, Derwin K. Commercially available extracellular matrix materials for rotator cuff repairs: state of the art and future trends. J Shoulder Elbow Surg 2007;16(5 Suppl):S171-8.

26. Derwin KA, Baker AR, Spragg RK, Leigh DR, Iannotti JP. Commercial extracellular matrix scaffolds for rotator cuff tendon repair. Biomechanical, biochemical, and cellular properties. J Bone Joint Surg Am 2006;88(12):2665-72.

27. Frazier SB, Roodhouse KA, Hourcade DE, Zhang L. The Quantification of Glycosaminoglycans: A Comparison of HPLC, Carbazole, and Alcian Blue Methods. Open Glycosci 2008;1:31-39.

28. Karlsson M, Bjornsson S. Quantitation of proteoglycans in biological fluids using Alcian blue. Methods Mol Biol 2001;171:159-73.

29. Stegemann H, Stalder K. Determination of hydroxyproline. Clin Chim Acta 1967;18(2):267-73.

30. Reddy GK, Enwemeka CS. A simplified method for the analysis of hydroxyproline in biological tissues. Clin Biochem 1996;29(3):225-9.

31. Hogan MV, Bagayoko N, James R, Starnes T, Katz A, Chhabra AB. Tissue Engineering Solutions for Tendon Repair. Journal of the American Academy of Orthopaedic Surgeons 2011;19(3):134-142.

32. Ferdous Z, Grande-Allen KJ. Utility and control of proteoglycans in tissue engineering. Tissue Engineering 2007;13(8):1893-1904.

33. Leigh DR, Abreu EL, Derwin KA. Changes in gene expression of individual matrix metalloproteinases differ in response to mechanical unloading of tendon fascicles in explant culture. J Orthop Res 2008;26(10):1306-12.

34. Meyer F, Wardale J, Best S, Cameron R, Rushton N, Brooks R. Effects of lactic acid and glycolic acid on human osteoblasts: A way to understand PLGA involvement in PLGA/calcium phosphate composite failure. Journal of Orthopaedic Research 2012;30(6):864-871.

35. Wren TAL, Yerby SA, Beaupre GS, Carter DR. Mechanical properties of the human Achilles tendon. Clinical Biomechanics 2001;16(3):245-251.

36. Lee DK. A preliminary study on the effects of acellular tissue graft augmentation in acute Achilles tendon ruptures. Journal of Foot & Ankle Surgery 2008;47(1):8-12.

37. Sabeh F, Ota I, Holmbeck K, Birkedal-Hansen H, Soloway P, Balbin M, Lopez-Otin C, Shapiro S, Inada M, Krane S and others. Tumor cell traffic through the extracellular matrix is controlled by the membrane-anchored collagenase MT1-MMP. Journal of Cell Biology 2004;167(4):769-781.

38. Collier IE, Legant W, Marmer B, Lubman O, Saffarian S, Wakatsuki T, Elson E, Goldberg GI. Diffusion of MMPs on the Surface of Collagen Fibrils: The Mobile Cell Surface - Collagen Substratum Interface. Plos One 2011;6(9).

39. Clark IA, Swingler TE, Sampieri CL, Edwards DR. The regulation of matrix metalloproteinases and their inhibitors. International Journal of Biochemistry & Cell Biology 2008;40(6-7):1362-1378.

CHAPTER 3: CO-CULTURED TISSUE-SPECIFIC SCAFFOLDS FOR TENDON/BONE INTERFACE ENGINEERING

INTRODUCTION

The tendon/ligament to bone interface, or enthesis has a complex structure/organization to enable transfer of forces through the tendon/ligament to the bone. The body naturally achieves force transition through a four layer gradient from tendon to fibrocartilage to mineralized fibrocartilage to bone[1-4]. Examples of tissues with an enthesis include the supraspinatus tendon of the shoulder rotator cuff and the anterior cruciate ligament in the knee[1,3]. Since these enthesis locations are mostly avascular, healing after injury is very limited and often requires surgical intervention to repair the damage. There are a reported 30,000-75,000 cases of rotator cuff repair per year in the United States[5] and an estimated 150,000 ACL surgeries each year[6]. In severe injuries to these sites a graft is necessary for repair[1,6-9].

Most grafts currently used clinically for repair are autograft or allograft but each has its own complications. Autografts have additional harvesting surgeries, donor site morbidity, and increased risk for infection, while allografts have complications with possible immune rejection, problems with cellular infiltration, and incorporation into the surrounding tissue environment[6,10-12]. Synthetic polymeric grafts have been used to investigate repair solutions in the ACL since the 1970s and showed good short term success but never integrated well into the repair site and ultimately failed[13-17]. Current, research using tissue engineering principles are widely reported using different biomaterials, cell types, and growth factors[18,19] . Focus has been to create different

conditions on a single scaffold that can be specific to multiple tissue types[20], such as muscle to tendon, cartilage to bone, and tendon/ligament to bone. This strategy can be implemented by changing the biomaterial's chemical or physical structure, the cell source or a growth factor signal specific to the targeted tissue, or any combination of the above[21].

Ultimately, regardless of tissue application, the scaffold will have to integrate into the tissue to transfer the loads of the musculoskeletal tissues to regain function[1]. Specifically in regards to this project, a tendon-to-bone repair scaffold will be made by modifying current commercially available degradable scaffold targeted for tendon repair with a tissue specific coating of co-cultured cell deposited extracellular matrix (ECM). Fibroblasts (FB) will be used to deposit "tendon" ECM and osteoblasts (OB) will be used to deposited "bone" ECM. In this study, we examine the formulation of co-culture medium for both cell types with regard to protein deposition and mineralization, seeding specificity on scaffold, and ECM characterization on the tissue specific regions of the scaffold.

METHODS

Medium Determination

To determine the appropriate co-culture medium formulation with respect to mineralization, NIH 3T3 mouse fibroblasts (CRL-1658 ATCC, Manassas, VA) or MC 3T3-E1 mouse calvarial osteoblasts (CRL-2593 ATCC, Manassas, VA) cells were seeded on tissue culture plastic (TCP) in single culture with varying concentrations of beta-glycerophosphate disodium pentahydrate (β-GP) (MPbio, Santa Ana, CA) to balance high OB mineralization with low FB mineralization. Both cell types were seeded at

$1x10^4$ cells/cm^2 per well in a 12-well plate(BD Falcon, San Jose, CA) in α-MEM (Hyclone, Waltham, MA) containing 10% fetal bovine serum (FBS) (Hyclone, Waltham, MA) + 1000 U/mL penicillin, 1000 µg/mL streptomycin, 2.5 µg/mL amphotericin-B (AB/AM) (Gibco, Grand Island, NY) and at every medium change 25 µg/mL L-ascorbic acid (AA) (Acros Organics, NJ) was freshly added. To this formulation 0, 1, 3, or 5 mM of β-GP was added. Medium was changed every 2-3 days. Seeded plates were cultured in an incubator at 37 °C and 5% CO_2. At timepoints of 1, 4, 7, and 14 days, medium was removed from the plates and samples were frozen at -80 °C until the end of the study, at which point 1 mL of biology grade water was added and all cells were lysed with an ultrasonic dismembrator (Fisher Scientific, Waltham, MA). Aliquots were then taken to perform picogreen assay for DNA quantification (Invitrogen, Grand Island, NY), Pierce BCA for total protein (ThermoScientific, Rockford, IL), and calcium assay for mineralization (Pointe Scientific, Canton, MI). All assays were performed according to the manufacturer's protocols. The medium determination experiment, including similar concentrations of medium additives and data collection timepoints were based on a similar study by Wang et al[2]. After the data were collected, total protein and mineralization data were normalized to DNA. All test medium formulations with each cell type were evaluated in triplicate at each time point.

Scaffold Seeding

The scaffold used for this study is X-Repair®, a commercially available poly-l-lactic acid (PLA) woven fabric provided by Synthasome Inc, CA. X-Repair® is currently used for surgical reinforcement for tendon rotator cuff repair. PLA fabric scaffolds were cut into strips with dimensions of 10 mm wide by 60 mm long. The edges were sealed by

thermally fusing the polymer so the fabric structure would not unravel. The scaffolds were cleaned with a detergent solution, rinsed thoroughly with deionized water multiple times, and sterilized with 70% ethanol and UV light. Prior to cell seeding, the scaffolds were soaked in sterile culture medium containing FBS overnight to aid in cell attachment. The scaffolds were seeded with FB and OB in co-culture at a $1x10^6$ cells/scaffold region, as shown in Figure 1. The total number of cells per scaffold was $2x10^6$, one million each of FB and OB. All seeded scaffolds were grown in α-MEM containing 10% FBS + AB/AM + 3mM β-GP and at every medium change 25 μg/mL AA was freshly added. All seeded scaffolds were kept in an incubator at 37°C and 5% CO_2.

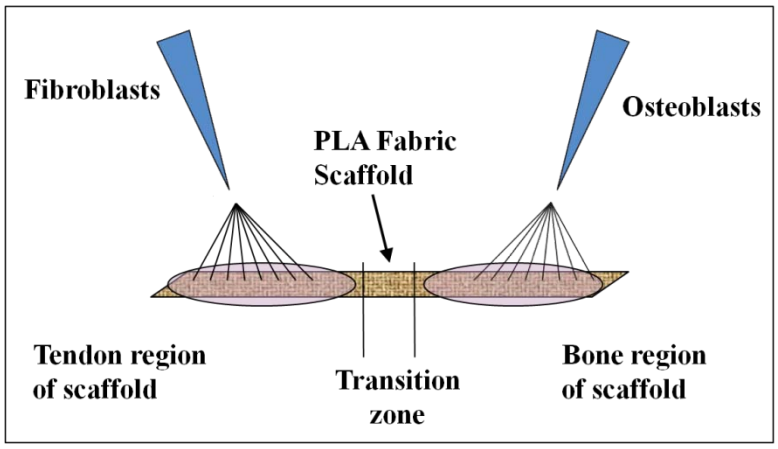

FIGURE 1. Schematic of how the PLA scaffolds are seeded with FB and OB on co-culture to make a tendon region and a bone region on the scaffold. There is a transition zone between the two regions where both cells interact.

Cell Tracking and Migration

To track the cells' location and migration after seeded and to confirm that tendon and bone regions can be successfully seeded on a scaffold, the cells were labeled with

two different fluorescent stains by a method modified by Wang et al[2]. FBs were labeled with Cell Tracker Green (Lonza, Alendale, NJ) and the OB were labeled with Cell Tracker Orange (Lonza, Alendale, NJ) according to the manufacturer's protocols. Briefly, cells were removed from the TCP flask, collected and centrifuged at 16,000xg for 5 minutes to form a pellet. FBs were resuspended in a 10 mM green tracker solution and the OB were resuspended in 10 mM orange tracker solution for 30 minutes and placed in an incubator. Labeled cells were seeded on the scaffolds as described previously, shown in Figure 1. The cells were allowed to attach to the scaffolds for 6 hours after seeding. The scaffolds were then placed in a sterile custom made cover glass petri dish for fluorescence imaging. Using an inverted microscope (Nikon, Melville, NY) and a motorized stage (ASI Imaging, Eugene, OR) the entire scaffold was imaged by taking approximately 200 images at 4x magnification and stitching the images into a montage using BioQuant Osteo software (BioQuant, Nashville, TN). Scaffolds were imaged once at excitation/emission (ex/em) of 470nm/515nm then again at ex/em of 540nm/590nm. Both images were then merged together with BioQuant. Images were replicated at 6, 18, 30, and 42 hours for cell migration.

ECM Deposition

Extracellular matrix on the scaffolds was quantified after 28 days culture to characterize and evaluate the matrix deposited by the cells on the scaffolds. Cells were seeded as previously described. The evaluated and selected culture medium used was α-MEM containing 10% FBS + AB/AM + 3mM β-GP and 25 μg/mL AA was freshly added at every medium change. All scaffolds were cultured individually in 100mm non-treated polystyrene petri dishes. Scaffolds were moved to new petri dishes every 7 days to

prevent cells that migrated off the scaffolds from becoming confluent. Scaffolds (n=4) were collected at timepoints of 1, 7, 14, 21 and 28 days. At each timepoint, the 10 x 60 mm scaffolds were removed from the petri dish and cut into three 10 x 20 mm sections. Each scaffold, therefore, produced a tendon section, a transition middle section, and a bone section for analysis. Each section was placed in a 1.5 mL microcentrifuge tube and 1 mL of a buffered enzymatic digestion solution of 100 μg/mL proteinase-K (Promega, Madison, WI) was added to every tube. All samples were then placed in an oven at 60°C overnight to digest the ECM. The following day phenylmethanesulfonylfluoride (PMSF) was added to a concentration of 5mM to inhibit the proteinase-K. All samples were homogenized using a sonic dismembrator and aliquots were removed for analysis. One aliquot was used to test for cell number through DNA quantification (Picogreen green assay, Invitrogen, Grand Island, NY). Another aliquot was used to measure the glycosaminoglycan (GAG) content (National Diagnostics, Atlanta, GA) through an alcian blue precipitation reaction[22,23]. The last aliquot was used to quantify collagen content through the detection of the amino acid hydroxyproline (HYP)[24,25]. All volumes were carefully recorded for normalization during analysis.

Statistics

The data for each test were collected and averaged. All assays including Pierce BCA, Calcium, GAG, and HYP were normalized to their respective picogreen DNA assays for each respective sample. Then Two-way ANOVA with Holm-Sidak post-hoc test was performed on the necessary groups at a significance level of $\alpha=0.05$ using SigmaStat 3.1 (Systat Software Inc., San Jose, CA).

RESULTS

This study had three main objectives: (1) to determine a suitable medium formulation to balance OB to FB mineralization, (2) to demonstrate successful substrate seeding in co-culture to create multiple regions on a single scaffold, and (3) to measure and quantify the ECM deposited across the scaffold and the difference in co-cultured regions.

Medium Determination

In the co-culture medium formulation, two additional components were added to the standard growth medium formulation, ascorbic acid for collagen deposition and β-GP for mineralization. Ascorbic acid concentration was held constant for all formulations at 25 μg/mL. The amount of β-GP was varied in the co-culture medium to look at differences in total protein expression and calcium deposition per cell by both FB and OB in single culture. Cell number was estimated from DNA measurements. Figure 2 shows that the FB did not differ significantly in total protein per cell regardless of β-GP concentration. There was only a gradual increase in protein deposition between days 1 and 14. The only significant difference is between day 1 and day 14 in the 5 mM group. The OB protein deposition was also not significantly affected by the β-GP. However, there were some significant time dependent increases in total protein compared to day 1. Overall, β-GP had little effect on total protein deposition which may be more strongly attributed to the ascorbic acid [26-28].

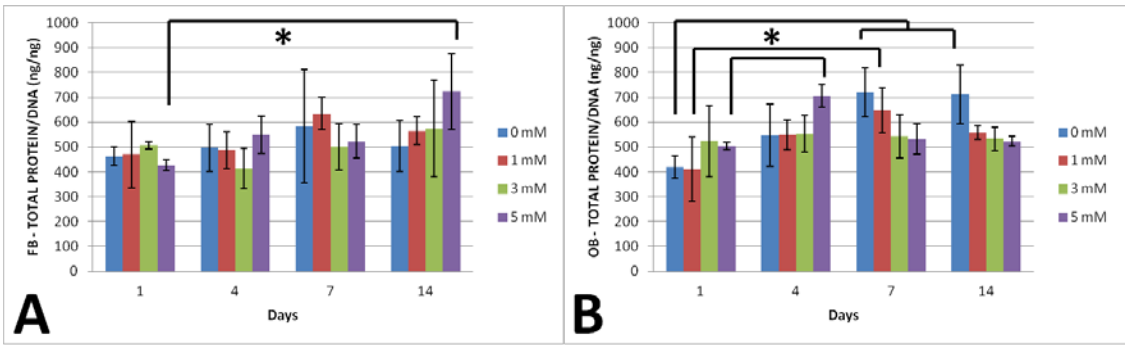

FIGURE 2. Average total protein deposition plus standard deviations of (A) FB and (B) OB cultured in 0, 1, 3, or 5 mM β-GP. Each group was measured in triplicate. There was no significant difference in FB or OB total protein deposition with regard to β-GP concentration. There are some significant time dependent effects on protein deposition. *****indicates statistical significance of $p<0.05$.

There was a more observable effect of β-GP concentration on mineralization in the OB cell line. Within days 1, 7, and 14, the 5mM β-GP concentration produced a significantly higher amount of calcium deposition than the other concentrations. There was also a significant time dependent increase (significance is not indicated in the OB graph) in calcium deposition for every β-GP concentration. There was no significant difference within each timepoint for β-GP concentration on FB mineralization. There was, however, a significantly higher amount of FB calcium deposition on the day 14 timepoint compared the other days, with the exception of the 3mM β-GP group. Due to the low fibroblast mineralization to osteoblast mineralization, the 3 mM β-GP concentration was used in medium formulations for the subsequent studies.

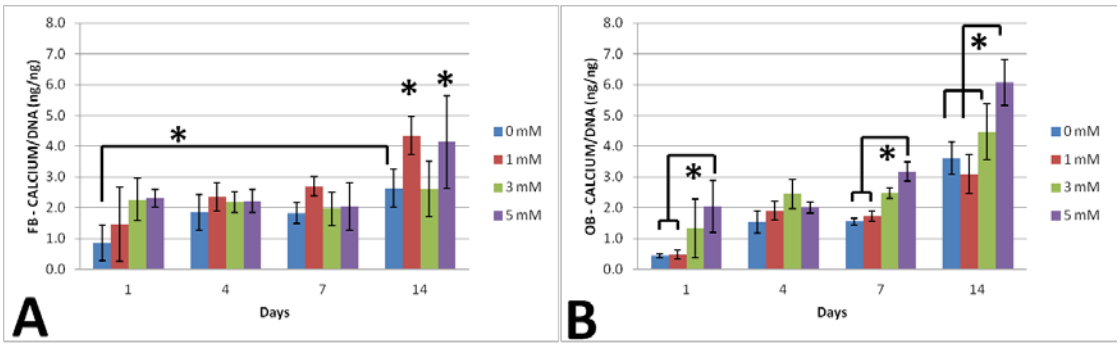

FIGURE 3. Average calcium deposition plus standard deviations of (A) FB and (B) OB cultured in 0, 1, 3, or 5 mM β-GP. Each group was measured in triplicate. There was not a significant difference between β-GP concentrations in FB mineralization. There was a significant time dependent increase in Day 14 compared to other days. For OBs, there was a significant increase in mineralization of the 5mM concentration for each time point compared to the other concentrations. There was also a significant increase in mineralization for all concentrations over time (not indicated on graph). *indicates statistical significance of $p<0.05$.

Fluorescence Imaging of Scaffold Seeding

The second objective of this study was to investigate seeding a single scaffold in co-culture to create tendon- and bone- specific regions. The FBs were stained with green tracking probe and the OBs were labeled with a red tracking probe. The montage image in Figure 4 shows the entire 10 mm by 60 mm scaffold first with the green filter enabled then with the red filter. Each montage is comprised of approximately 200 individual 4x magnification images taken with the aid of a motorized stage and stitched together using BioQuant software. As can be seen in Figure 4, both FB and OB are attached on their respective half of the scaffold creating the tissue specific regions. The general tissue specific regions at low magnification are easier to distinguish. Figure 5 contains the two non-merged images with smaller selected regions shown at higher magnifications. There are very few FB in the OB region and vice versa. On the left hand edge of the OB side, FB did attach and is more evident at higher exposure times. However, most cells are

located in their respective regions with a decreasing gradient across the scaffold. There was no noticeable migration of cells between regions observed over the 42 hours in Figure 6. The fluorescence label loses intensity over time, and therefore, the exposure time was increased by the 42 hour image to intensify the colors on the scaffold. Because of the increased exposure, the 42 hour image has a noticeable amount of unanticipated autofluorescence in the periphery of the image. This is due to the cyanoacrylate used to make the custom glass cover slip petri dish for imaging and not the FB fluorescing.

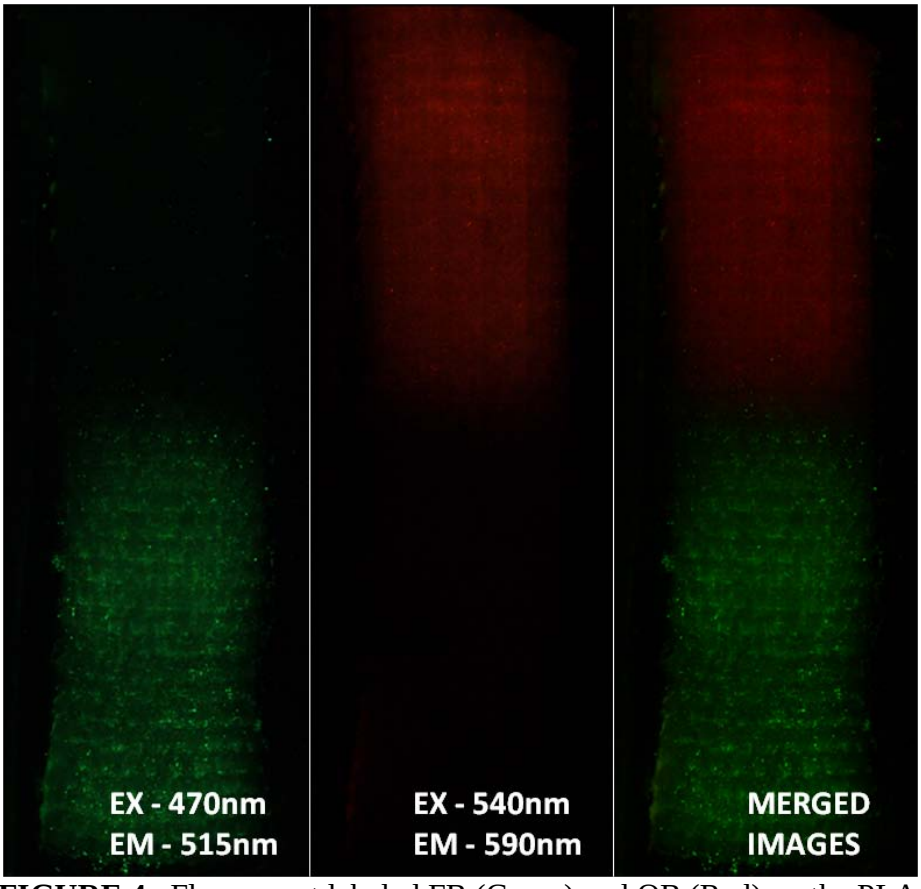

FIGURE 4. Fluorescent labeled FB (Green) and OB (Red) on the PLA scaffold form distinct tissue specific regions at 6 hours. The two images using the cell tracker green and cell tracker orange probes separately were merged to show how the cells are seeded on the over entire scaffold. Image consists of approximately 200 images at 4x magnification stitched together. Scaffold size is 10 mm wide by 60 mm long.

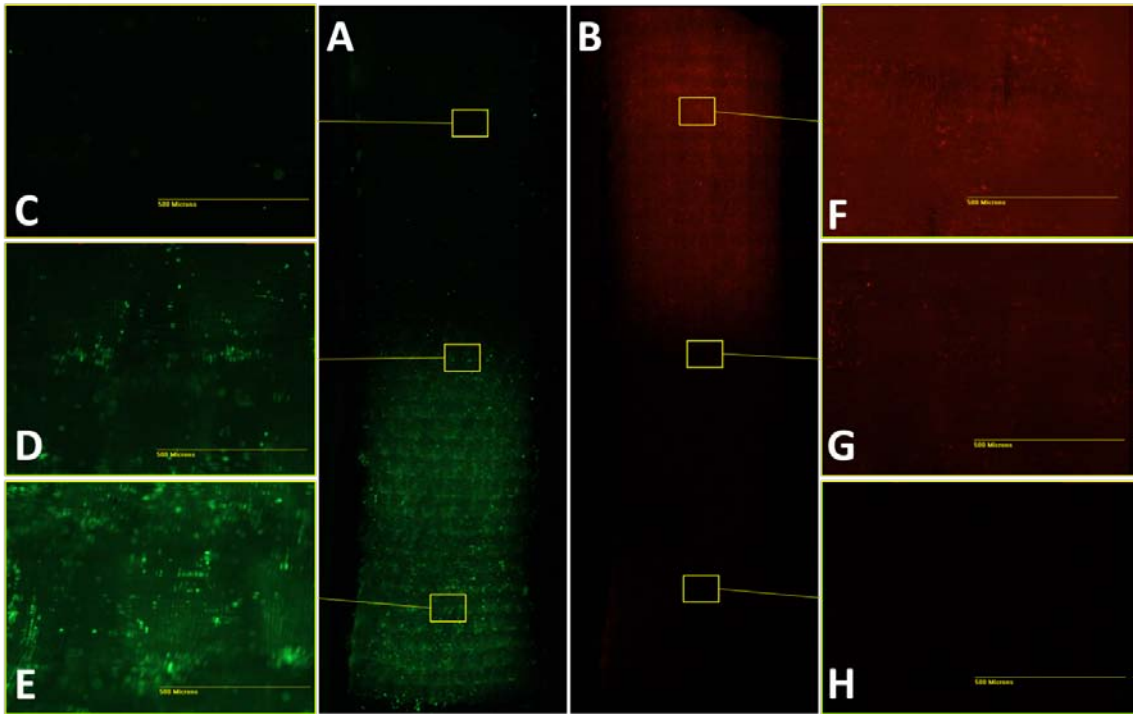

FIGURE 5. Image A and B The same two images seen from Figure 4 with higher magnification selections shown. Images C, D, and E show FB in the bone, transition, and tendon regions, respectively. Images F, G, and H show OB in the bone, transition, and tendon regions, respectively.

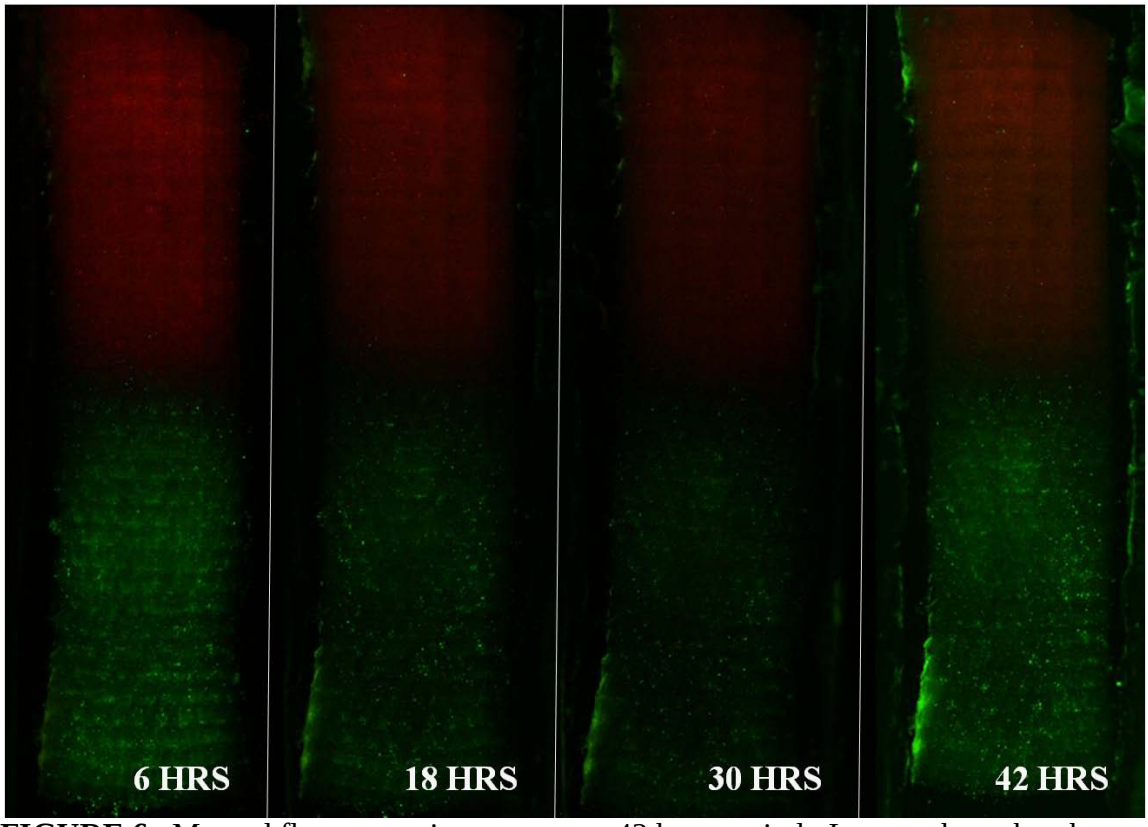

FIGURE 6. Merged fluorescent images over a 42 hour period. Images show that the cells maintain the tissue specific regions on the scaffold. No noticeable migration was observed in the measured time frame. There are green labeled FB in the bone region and red labeled OB in the tendon region even though no major cell migration was observed.

ECM Deposition

The last objective of this study was to quantify the basic components of the ECM deposited on the static scaffolds in the tendon, bone, and transition regions. These components are GAGs and collagen measured by alcian blue and hydroxyproline, respectively. Deposited matrix distribution among the different regions the scaffold was measured by analyzing equal thirds of the scaffold, creating a tendon, transition, and bone specimen per scaffold. The DNA quantified in Figure 7, indicated no significant differences between particular sections representing uniform cell dispersal over the

scaffold, including the transition section. A significant time- dependent difference between day 1 and the other timepoints was found. DNA was used to normalize the GAG and HYP data. GAG/DNA measurement was significantly higher in the tendon region compared to the other regions on day 14 and day 28. No significant collagen deposition difference between scaffold regions was determined in these static conditions. A continual and significantly increasing deposition of collagen over the entire 28 day study was found. This indicates good cell viability and activity on the scaffold. Even though not statistically significant, an interesting observation was that the ECM detected in the transition region had intermediate values in between the bone and tendon regions and would suggest mixed contributions from each cell type on the scaffold.

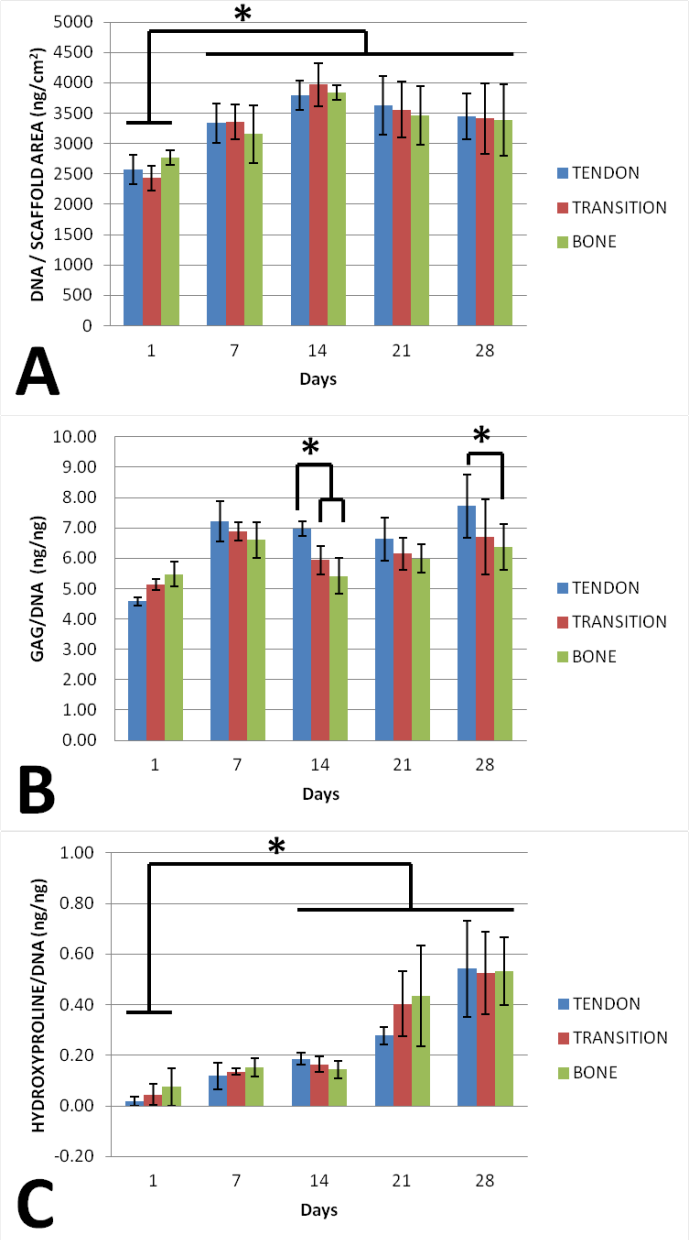

FIGURE 7. Quantification of DNA, GAG, and HYP deposition on the co-cultured scaffolds. The scaffolds were sectioned into equal thirds and analyzed separately. All data are mean values plus standard deviations. Groups were tested with n=4 replicates. (A) DNA amounts were not significantly different between the scaffolds regions but it did significantly increase from day 1 then stay relatively constant. (B) There was a significantly higher deposition for GAG/DNA in the tendon region compared to the bone region for day 14 and 28, with the transition region having intermediate values between the two. (C) There were no significant differences between groups for HYP/DNA deposition but there was significantly increasing collagen content over time. Continually increasing collagen deposition is indicative of active and viable cells on the scaffold, in this co-culture model. *indicates statistical significance of $p<0.05$.

DISCUSSION

The ultimate goal of this research was to create a more effective tissue engineered scaffold for tendon to bone interfaces that will integrate with the host tissue, provide functional aid while healing, and then degrade overtime as the host tissue replaces the scaffold. The approach taken to achieve this goal was to create a tendon specific and a bone specific region on a scaffold using cell deposited ECM on a degradable PLA fabric scaffold. For the tendon region fibroblasts were used and for the bone region osteoblasts were cultured on the scaffold. In this study specifically, a co-culture compatible medium formulation was determined, the PLA fabric scaffold can be seeded in a way to create two different tissue-specific regions on the scaffold, and deposited ECM in each specific region including a transition zone was quantified.

Other studies have taken similar approaches to repair of musculoskeletal interfaces. Synthetic degradable polymers and ECM components are common scaffold choices for tendon/ligament tissue engineering due to control of factors such as mechanical properties, pore sizes, degradation properties, and scaffold geometry[6,21,29-32]. For example, to have soft tissue ingrowth into a scaffold a minimum pore size of 200 μm has been suggested, while calcified tissue needs a minimum of 100 μm. Another approach to engineering interfaces is changing the cell type involved with the scaffold. Osteoblasts are common for bone tissue engineering and specialized tendon fibroblasts, called tenocytes, have been used for tendon. Tenocytes deposit tendon-specific ECM, but tenocytes also have low metabolic activity and low healing capabilities which are used for maintenance and not necessarily regeneration[9,11]. Therefore, other fibroblasts, including dermal fibroblasts, have been investigated as well [33]. After choosing individual

cell types for the appropriate ECM deposition, introducing the cells into a co-culture environment could modify the ECM deposition compared to a single culture. In one published study by Wang et al., they looked at how osteoblasts and fibroblasts interact in a co-culture system for a ligament to bone interface, including preliminary experiments to determine medium composition and ECM deposition of the co-cultured multiphase set-up[2] similar to our studies.

The medium formulation of Wang et al., found that 1mM β-GP was optimal for low fibroblast mineralization and retained osteoblast mineralization at 7 or 14 days[2]. We found that 3mM β-GP provided low fibroblast to osteoblast mineralization. This response is most likely cell line specific. In their study primary bovine cells were used[2], in comparison, we used well characterized mouse cell lines, NIH 3T3 and MC 3T3[26]. The co-culture medium should be tuned to each unique tissue engineering system because ECM and mineralization deposition could have impacts on scaffold integration with tissues. For this application, the osteoblast seeded bone region was targeted for higher mineralization than the fibroblast seeded tendon region. It was hypothesized that the higher mineral content on the bone side would help provide an environment for anchoring the scaffold in the bone. This approach is a common technique for bone tissue engineering which uses minerals like di- and tri-calcium phosphates, or hydroxyapatites to signal osteointegration[34,35]. Conversely, a low mineralized tendon region is also a functional need. Native tendon is fibrous and non-calcified lending to predominantly tensile loading while bone being highly calcified acts mostly in compression [36]. Conditioning each region properly could help achieve functional loading earlier after implantation.

Mineralization is not the only important component to the tendon-to-bone junction; subtle changes in ECM composition, like elastin, collagens, proteoglycans, and GAGs also play a role. It was observed that the deposition of ECM transition zone on our PLA scaffold had average values that were in between the bone region and tendon regions values with respect to GAG and collagen. This finding would indicate that the ECM deposition in the center of the scaffold is a mix of osteoblast and fibroblast expression. These initial findings in validating this ECM deposition approach have shown promise in establishing tissue specific regions with a small transition. In future studies planned identification of more specific changes with respect to tendon-specific and bone-specific ECM deposition will be investigated. Other reported tendon/ligament bone studies have shown how a fibroblast and osteoblast co-cultured scaffold can form transitions with characteristics of native tissue between regions. Wang et al. showed that in a co-cultured fibroblast and osteoblast environment an increased collagen type II ECM, representative of a cartilaginous zone, was deposited without the presence of cartilage forming cells[2]. Their approach was taken a step further to include chondrocytes. Several successive studies by Spalazzi et al, using degradable multiphasic scaffolds with controlled porosity and a tri-culture of fibroblasts, chondrocytes, and osteoblasts measured interface specific ECM components *in vitro* and *in vivo* to understand the role of multiple tissue types in a single scaffold[12,37,38]. They have demonstrated the ECM of the ligament, fibrocartilage, and bone regions found at the enthesis can be partially recreated with *in vitro* culture. While no functional mechanical data of the tri-phasic scaffolds were reported these experiments are valuable to understanding how cells can interact spatially to produce ECM of the enthesis. In contrast, Ma et al, proposes that

because neo-tissue genesis in a tissue engineering process is not exactly the same as developmental or wound healing, it is likely unnecessary and impractical for a tissue engineered scaffold to completely duplicate the ECM[29]. Therefore, an effective therapy may not need to fully recreate the tendon, fibrocartilage, and bone ECM *in vitro*, but deposit sufficient specific ECM to direct tissue integration *in vivo*. The production of a functional repair of the enthesis may need to gain short-term mechanical stability of the scaffold in order to initiate mechanical loading while the long-term integration of the scaffold is directed by signaling of the tendon-specific and bone-specific ECM coatings. A reported study by Encalada-Diaz et al. suggests in the rotator cuff a short-term stability with long-term integration may be the case[39].

Previous studies with non-degradable fabric PET scaffolds showed very good short term results in ACL repair, but were not able to achieve long-term integration with the surrounding tissues[13-17]. Applying a tissue-specific ECM coating may help bridge the gap between the short-term success of polymer grafts and the long-term integration of biologic materials[17,40]. For example Recently Li et al., has modified PET ligament scaffolds with bioglass and hydroxyapatite to try and increase osseointegration of the scaffold into the bone[41]. They performed an *in vivo* bone tunnel study for 2 weeks and showed evidence of initial scaffold integration; however, long-term integration was not evaluated in their study. The degradable X-repair PLA scaffold used in our studies potentially has an additional advantage over a non-degradable scaffold of slowly resorbing over a long-term period while still having short-term mechanical stability necessary for some functional loading. The tissue-specific ECM coatings deposited on the PLA scaffold may help integration with the surrounding tissues for successful long-

term integration. Eventual investigation with a functional animal model will be necessary to fully address this hypothesis.

In conclusion, the steps taken in this study have aimed to create a cell specific extracellular matrix environment on a mechanically robust degradable scaffold to enable better fixation of tendinous soft tissues at bony interfaces. The outlined approach is to produce tissue-preferred areas on a scaffold to target the native tissues to integrate with the scaffold. The scaffold will then assist with mechanical loading while the co-cultured ECM aids the bodies healing to remodel the wound. To achieve this goal, we have selected a suitable co-culture medium formulation for our initial work with the enthesis scaffold. We were able to seed the scaffold in co-culture to create two distinct tissue specific regions on the scaffold. Lastly, we measured ECM deposition on three regions of the scaffold. Our future work is to increase the specificity of the ECM coating through mechanical stimulation of the cell seeded scaffolds while depositing ECM and perform more specific ECM analysis.

ACKNOWLEDGEMENTS/FUNDING

We would like to thank Synthasome, Inc for generous donations of X-repair PLA fabric. We also thank Jessica Jennings, PhD, at University of Memphis for help with fluorescence microscopy.

This project was funded by the DOD PRORP- USAMRMC W81XWH-10-1-0768 grant and by the Biomaterials Applications of Memphis (BAM) Laboratories in the Biomedical Engineering Department at the University of Memphis.

REFERENCES

1. Zhang X, Bogdanowicz D, Erisken C, Lee NM, Lu HH. Biomimetic scaffold design for functional and integrative tendon repair. J Shoulder Elbow Surg;21(2):266-77.

2. Wang IE, Shan J, Choi R, Oh S, Kepler CK, Chen FH, Lu HH. Role of osteoblast-fibroblast interactions in the formation of the ligament-to-bone interface. J Orthop Res 2007;25(12):1609-20.

3. Benjamin M, Milz S, Bydder GM. Magnetic resonance imaging of entheses. Part 1. Clin Radiol 2008;63(6):691-703.

4. Dourte LM, Kuntz AF, Soslowsky LJ. Twenty-five years of tendon and ligament research. J Orthop Res 2008;26(10):1297-305.

5. Ricchetti ET, Aurora A, Iannotti JP, Derwin KA. Scaffold devices for rotator cuff repair. Journal of Shoulder and Elbow Surgery 2012;21(2):251-265.

6. Cooper JA, Lu HH, Ko FK, Freeman JW, Laurencin CT. Fiber-based tissue-engineered scaffold for ligament replacement: design considerations and in vitro evaluation. Biomaterials 2005;26(13):1523-32.

7. Hashimoto Y, Yoshida G, Toyoda H, Takaoka K. Generation of tendon-to-bone interface "enthesis" with use of recombinant BMP-2 in a rabbit model. J Orthop Res 2007;25(11):1415-24.

8. Joshi SD, Webb K. Variation of cyclic strain parameters regulates development of elastic modulus in fibroblast/substrate constructs. J Orthop Res 2008;26(8):1105-13.

9. Abousleiman RI, Reyes Y, McFetridge P, Sikavitsas V. Tendon tissue engineering using cell-seeded umbilical veins cultured in a mechanical stimulator. Tissue Eng Part A 2009;15(4):787-95.

10. Soon MY, Hassan A, Hui JH, Goh JC, Lee EH. An analysis of soft tissue allograft anterior cruciate ligament reconstruction in a rabbit model: a short-term study of the use of mesenchymal stem cells to enhance tendon osteointegration. Am J Sports Med 2007;35(6):962-71.

11. Kuo CK, Marturano JE, Tuan RS. Novel strategies in tendon and ligament tissue engineering: Advanced biomaterials and regeneration motifs. Sports Med Arthrosc Rehabil Ther Technol;2:20.

12. Spalazzi JP, Dagher E, Doty SB, Guo XE, Rodeo SA, Lu HH. In vivo evaluation of a multiphased scaffold designed for orthopaedic interface tissue engineering and soft tissue-to-bone integration. J Biomed Mater Res A 2008;86(1):1-12.

13. Guidoin R, Poddevin N, Marois Y, King MW, Belanger AY, Stroman P, Cronier B, Delagoutte JP, Maynard D, Benichoux R and others. Mechanisms of Failure for Anterior Cruciate Ligament Prostheses Implanted in Humans - a Retrospective Analysis of 79 Surgically Excised Explants. Polymers & Polymer Composites 1995;3(2):79-97.

14. Jenny JY, Jenny G, Daubresse F. Replacement of the Anterior Cruciate Ligament with Three Different Dacron Prostheses. International Orthopaedics 1991;15(1):23-28.

15. Seitz H, Marlovits S, Schwendenwein I, Muller E, Vecsei V. Biocompatibility of polyethylene terephthalate (Trevira (R) hochfest) augmentation device in repair of the anterior cruciate ligament. Biomaterials 1998;19(1-3):189-196.

16. Seitz H, Lang S, Marlovits S, Mousavi M, Kolonja A. Repair of the anterior cruciate ligament - a morphological study in sheep. Medizinische Welt 1998;49(12):610-617.

17. Guidoin MF, Marois Y, Bejui J, Poddevin N, King MW, Guidoin R. Analysis of retrieved polymer fiber based replacements for the ACL. Biomaterials 2000;21(23):2461-2474.

18. Lu HH, Jiang J. Interface tissue engineering and the formulation of multiple-tissue systems. Adv Biochem Eng Biotechnol 2006;102:91-111.

19. Lu HH, Subramony SD, Boushell MK, Zhang X. Tissue engineering strategies for the regeneration of orthopedic interfaces. Ann Biomed Eng 2010;38(6):2142-54.

20. Zhang YY, He YJ, Bharadwaj S, Hammam N, Carnagey K, Myers R, Atala A, Van Dyke M. Tissue-specific extracellular matrix coatings for the promotion of cell proliferation and maintenance of cell phenotype. Biomaterials 2009;30(23-24):4021-4028.

21. Yang PJ, Temenoff JS. Engineering orthopedic tissue interfaces. Tissue Eng Part B Rev 2009;15(2):127-41.

22. Frazier SB, Roodhouse KA, Hourcade DE, Zhang L. The Quantification of Glycosaminoglycans: A Comparison of HPLC, Carbazole, and Alcian Blue Methods. Open Glycosci 2008;1:31-39.

23. Karlsson M, Bjornsson S. Quantitation of proteoglycans in biological fluids using Alcian blue. Methods Mol Biol 2001;171:159-73.

24. Stegemann H, Stalder K. Determination of hydroxyproline. Clin Chim Acta 1967;18(2):267-73.

25. Reddy GK, Enwemeka CS. A simplified method for the analysis of hydroxyproline in biological tissues. Clin Biochem 1996;29(3):225-9.

26. Wang D, Christensen K, Chawla K, Xiao GZ, Krebsbach PH, Franceschi RT. Isolation and characterization of MC3T3-E1 preosteoblast subclones with distinct in vitro and in vivo differentiation mineralization potential. Journal of Bone and Mineral Research 1999;14(6):893-903.

27. Chepda T, Cadau M, Girin P, Frey J, Chamson A. Monitoring of ascorbate at a constant rate in cell culture: Effect on cell growth. In Vitro Cellular & Developmental Biology-Animal 2001;37(1):26-30.

28. Geesin JC, Darr D, Kaufman R, Murad S, Pinnell SR. Ascorbic-Acid Specifically Increases Type-I and Type-Iii Procollagen Messenger-Rna Levels in Human-Skin Fibroblasts. Journal of Investigative Dermatology 1988;90(4):420-424.

29. Ma PX. Biomimetic materials for tissue engineering. Advanced Drug Delivery Reviews 2008;60(2):184-198.

30. Derwin KA, Codsi MJ, Milks RA, Baker AR, McCarron JA, Iannotti JP. Rotator cuff repair augmentation in a canine model with use of a woven poly-L-lactide device. J Bone Joint Surg Am 2009;91(5):1159-71.

31. Visser LC, Arnoczky SP, Caballero O, Kern A, Ratcliffe A, Gardner KL. Growth factor-rich plasma increases tendon cell proliferation and matrix synthesis on a synthetic scaffold: an in vitro study. Tissue Eng Part A 2010;16(3):1021-9.

32. Moffat KL, Kwei ASP, Spalazzi JP, Doty SB, Levine WN, Lu HH. Novel Nanofiber-Based Scaffold for Rotator Cuff Repair and Augmentation. Tissue Engineering Part A 2009;15(1):115-126.

33. Deng D, Liu W, Xu F, Yang Y, Zhou G, Zhang WJ, Cui L, Cao Y. Engineering human neo-tendon tissue in vitro with human dermal fibroblasts under static mechanical strain. Biomaterials 2009;30(35):6724-30.

34. Khan Y, Yaszemski MJ, Mikos AG, Laurencin CT. Tissue engineering of bone: material and matrix considerations. J Bone Joint Surg Am 2008;90 Suppl 1:36-42.

35. Narayanan R, Seshadri SK, Kwon TY, Kim KH. Calcium phosphate-based coatings on titanium and its alloys. J Biomed Mater Res B Appl Biomater 2008;85(1):279-99.

36. Moffat KL, Wang IN, Rodeo SA, Lu HH. Orthopedic interface tissue engineering for the biological fixation of soft tissue grafts. Clin Sports Med 2009;28(1):157-76.

37. Spalazzi JP, Dagher E, Doty SB, Guo XE, Rodeo SA, Lu HH. In vivo evaluation of a tri-phasic composite scaffold for anterior cruciate ligament-to-bone integration. Conf Proc IEEE Eng Med Biol Soc 2006;1:525-8.

38. Spalazzi JP, Doty SB, Moffat KL, Levine WN, Lu HH. Development of controlled matrix heterogeneity on a triphasic scaffold for orthopedic interface tissue engineering. Tissue Eng 2006;12(12):3497-508.

39. Encalada-Diaz I, Cole BJ, MacGillivray JD, Ruiz-Suarez M, Kercher JS, Friel NA, Valero-Gonzalez F. Rotator cuff repair augmentation using a novel polycarbonate polyurethane patch: preliminary results at 12 months' follow-up. Journal of Shoulder and Elbow Surgery 2011;20(5):788-794.

40. Zantop T, Gilbert TW, Yoder MC, Badylak SF. Extracellular matrix scaffolds are repopulated by bone marrow-derived cells in a mouse model of achilles tendon reconstruction. J Orthop Res 2006;24(6):1299-309.

41. Li H, Wu Y, Ge Y, Jiang J, Gao K, Zhang P, Wu L, Chen S. Composite coating of 58S bioglass and hydroxyapatite on a poly (ethylene terepthalate) artificial ligament graft for the graft osseointegration in a bone tunnel. Applied Surface Science;257(22):9371-9376.

CHAPTER 4: MECHANICALLY-STIMULATED CO-CULTURED TISSUE-SPECIFIC SCAFFOLDS FOR TENDON/BONE INTERFACE ENGINEERING

INTRODUCTION

The tendon/ligament to bone interface, or enthesis, is a complex transition that is essential for functional motion as the interface enables the transfer of loads through the musculoskeletal system. The musculoskeletal enthesis is a continuous transition from tendon to fibrocartilage to mineralized fibrocartilage to bone[1-4] as observed at the supraspinatus tendon of the shoulder rotator cuff and the anterior cruciate ligament in the knee[1,3]. These sites are considered avascular, limiting the healing after injury and often requiring surgery for functional repair[1,5,6]. Tissue engineering is a mix of biomaterials, cells, and biologic signals that can offer a solution for enthesis repair[7-9]. However, studies have shown that specific minutiae in selecting the tissue engineering factors can have impacts on the how the tissues are regenerated[10,11]. For example, increasing the pore size greater than 150 microns will allow bone tissues to form in the biomaterial and tendon tissues require pore sizes greater the 250 microns to form[5]. Different cells types like fibroblasts, osteoblasts, or chondrocytes deposit their own extracellular matrix (ECM) components differing in collagen types and amounts [12-14]. Finally, the effects of combinations of growth factors and cytokine signaling can be powerful determinants of the tissue type formed *in vivo*. For example, bone morphogenetic protein-2 (BMP-2) can induce bone formation in a muscle pouch where bone is not naturally found[15]. These types of growth factors and signals can be useful tools for tissue engineering.

One signaling tool for tissue formation that is commonly overlooked is mechanical stimulation. The classic example of how mechanical forces can affect tissues is Wolff's law in bone[16]. Essentially, bone will remodel according to the forces acting upon the bone, so increases in cyclic forces will cause cells to produce more bone and decreases in stimulation will lead to bone resorption. There is a similar response in tendon and other soft tissues such as muscle where an increase in use will lead to an increase in mass and ultimate strength while a decrease in use will lead to a decrease in mass and tensile strength[17] . Techniques of applying mechanical stimulation to tissues have been used in muscle and cardiac tissue engineering[18,19]. To apply these mechanical strains, systems need to be developed to accurately control the forces applied, strain rates, number of cycles, temperature, and gas and nutrient exchange while remaining sterile[18]. How these parameters are actually controlled varies and several researchers have taken on the challenge of creating mechanical bioreactors to understand the role of mechanical stimulation in tissue engineering[6,18-25]. Results from mechanical bioreactor studies have determined that the strains, rates, number of cycles, and resting periods can all affect the type of ECM deposited[6,18-25]. These effects are most likely specific to each cell type and biomaterial scaffold used in the mechanical bioreactor.

In this study, co-cultured tendon-to-bone scaffolds were mechanically stimulated in a custom designed bioreactor for 35 days. It is hypothesized that cyclic mechanical stimulation during ECM formation will increase collagen deposition and alignment on a fabric substrate and the deposited ECM will cause an increase in tissue specific gene markers when mesenchymal stem cells (MSCs) are exposed to the ECM. A commercially available degradable poly-l-lactic acid (PLA) scaffold targeted for tendon

repair was stretched over 35 days in a custom built dual strain bioreactor. Fibroblasts were used to deposit "tendon" ECM and osteoblasts were used to deposit "bone" ECM. Fibroblast and osteoblast deposited ECM was examined histologically and compared to determine the effects of mechanical strain on the morphology and type of ECM produced. Once the ECM was deposited on the scaffold, rat (MSCs) were exposed to the ECM coating and tissue-specific gene activation was measured. The ECM of the scaffolds was then characterized through quantitative assays and histological analysis.

METHODS

Scaffold Seeding

The tendon repair scaffold used for this study is X-Repair®, a commercially available poly-l-lactic acid (PLA) woven fabric provided by Synthasome Inc, CA. X-Repair® is currently used for surgical reinforcement for tendon rotator cuff repair. All scaffolds in this study were seeded using the following protocol. PLA fabric scaffolds were cut into strips with dimensions of 10 mm wide by 80 mm long. The edges were sealed by thermally fusing the polymer so the fabric structure would not unravel. The scaffolds were cleaned with a detergent solution, rinsed thoroughly with deionized water multiple times, and sanitized with 70% EtOH and UV light. Prior to cell seeding, the scaffolds were soaked in sterile culture medium containing fetal bovine serum (formulation described below) overnight to aid in cell attachment. The scaffolds were seeded with NIH 3T3 fibroblasts (FB) and MC 3T3 osteoblasts (OB) in co-culture at a $1x10^6$ cells/scaffold region, shown in Figure 1. The total number of cells per scaffold is $2x10^6$, one million each of FB and OB. All seeded scaffolds were cultured in α-MEM (Hyclone, Waltham, MA) containing 10% fetal bovine serum (FBS) (Hyclone, Waltham,

MA) + 1000 U/mL penicillin, 1000 µg/mL streptomycin, 2.5 µg/mL amphotericin-B (Gibco, Grand Island, NY) + 3 mM of beta glycerophosphate(β-GP) and 25 µg/mL L-ascorbic acid (AA) (Acros Organics, NJ). All seeded scaffolds were kept in an incubator at 37°C and 5% CO_2 for 24 hours prior to placement in the bioreactor.

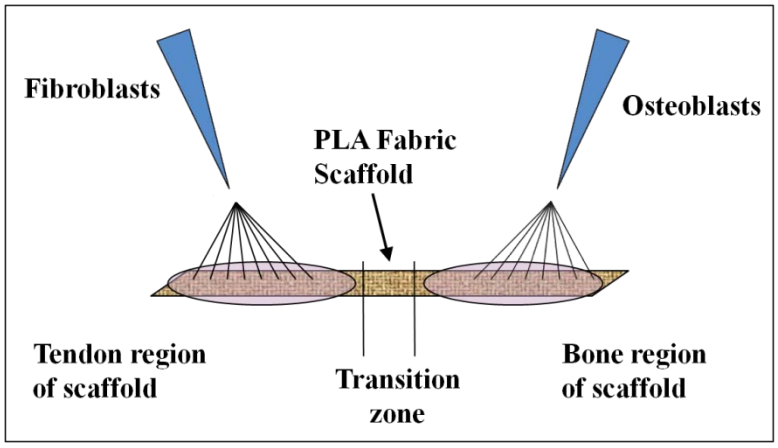

FIGURE 1. Schematic of how the PLA scaffolds are seeded with fibroblasts and osteoblasts on co-culture to make a tendon region and a bone region on the scaffold. There is a transition zone between the two regions where both cells interact.

Bioreactor and Mechanical Stimulation

After samples were seeded they were placed in the bioreactor pictured in Figure 2. Two separate chambers were used each with 4 scaffolds per chamber. The FB side of the scaffold was placed between the clamps labeled in Figure 2 as (A) and the OB was placed in section (B). One chamber had the adjustable center clamp intact which stretched the (A) FB region but not the (B) OB region (now termed FB STIM). These scaffolds were cultured for 21 days with the middle clamp intact then the clamp was removed to allow the cells to infiltrate the transition region to deposit ECM and the entire scaffold were

stimulated for a further 14 days. In the second chamber the center clamp was never utilized which allowed for the entire scaffold to be stimulated for all 35 days (termed FB + OB STIM). A stretching regime of 5% cyclic strain at 0.5 Hz for 1 hour per day every day was used for the length study. The culture medium formulation was α-MEM + 10% FBS + 1000 U/mL penicillin, 1000 μg/mL streptomycin, 2.5 μg/mL amphotericin-B + 3 mM of β-GP and biweekly 25 μg/mL AA was freshly added. Medium was completely refreshed every 7 days. Both chambers were kept in an incubator at 37 °C and 5% CO_2. At 35 days, scaffolds were removed from the chamber and decellularized for MSC seeding.

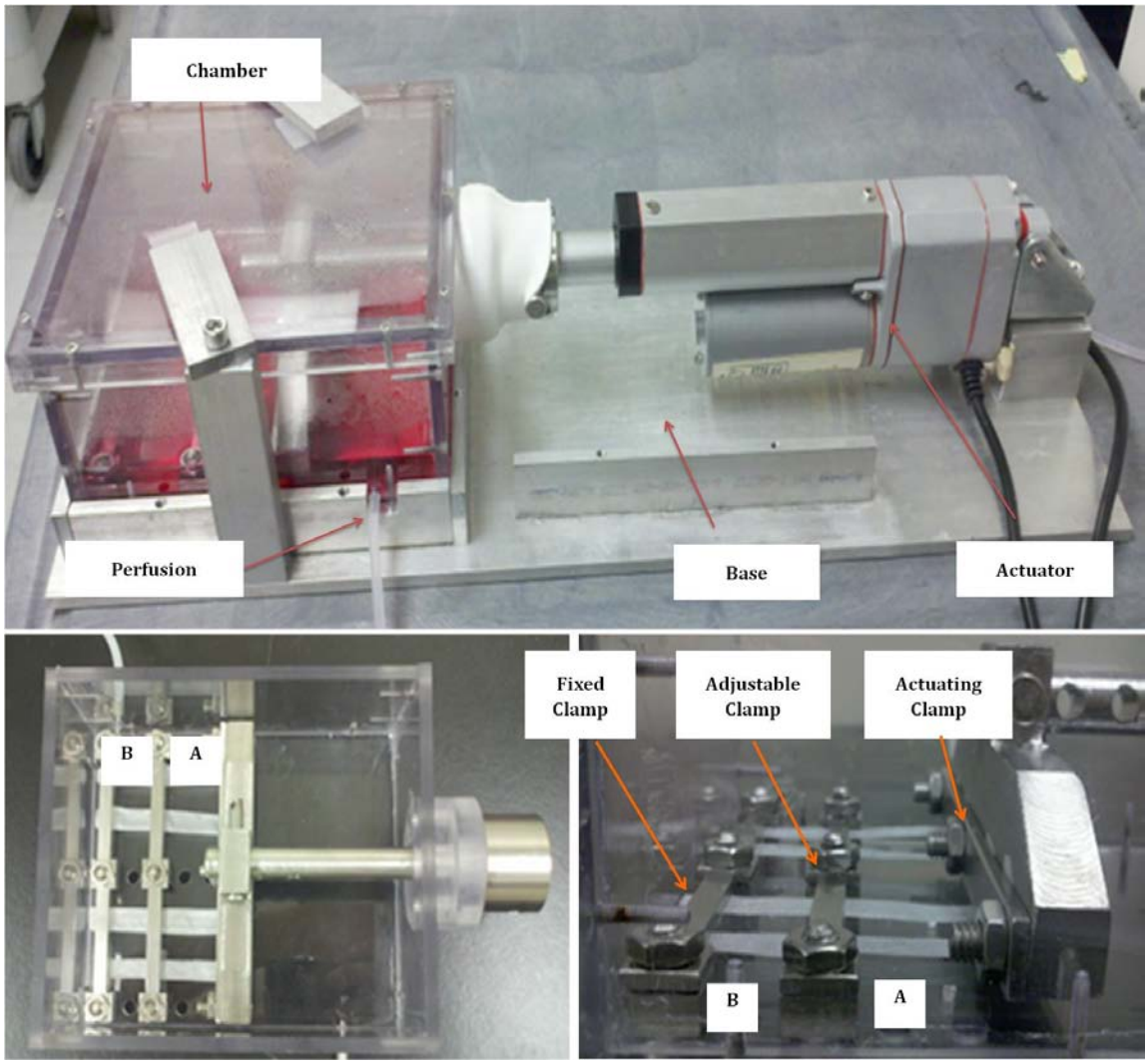

FIGURE 2. Images of the custom designed bioreactor used for the mechanical stimulation studies. The top image shows the sterile chamber connected to the linear actuator with gas permeable medium circulation lines attached. The bottom left image shows a top down view of the inside of the chamber with the actuator arm connected to the clamps that hold the scaffolds. The bottom right image shows the section labeled (A) between the actuating clamp and the center adjustable clamp receives mechanic stimulation and the section labeled (B) between the center adjustable clamp and the fixed clamp does not receive stimulations. The fibroblast seeded region of the scaffold is placed in (A) and the osteoblast seeded region is placed in (B). The entire chamber and actuator fits inside of an incubator maintained at 37°C and 5% CO_2.

Decellularization and Mesenchymal Stem Cell Seeding

At the end of the 35 days the 10 x 80 mm scaffolds were removed from the chambers and cut into three equal sections. Each scaffold, therefore, produced a tendon section, a transition middle section, and a bone section for analysis. Scaffolds were decellularized to remove any fibroblasts or osteoblasts on the scaffolds prior to MSC seeding. The decellularization protocol was a mixture of freeze thaw, hypo- and hyper-ionic solutions. First samples were frozen at -80C, thawed and repeated. The samples were alternated in solutions of deionized (DI) water for 1 hour and 10x phosphate buffered solution (PBS) for 1 hour. This cycle was repeated for 6 cycles, placed in DI water for one more hour, then soaked in 1x PBS for 1 hour prior to cell seeding.

Primary rat mesenchymal stem cells (MSC) were isolated from rat femurs as previously described[26]. These cells were expanded then used at passage 6. MSCs were seeded on each scaffold section at $1x10^6$ cells per section (n=3). MSCs were also seeded on tissue culture plastic (TCP) as a control (n=3). Samples and cells were cultured in α-MEM containing 10% FBS + 1000 U/mL penicillin, 1000 μg/mL streptomycin, 2.5 μg/mL amphotericin-B (Gibco, Grand Island, NY) for 24 hours. After the 24 hour seeding time, scaffolds sections were placed in a sterile PCR grade 1.5 mL centrifuge tube and submerged in 0.25% trypsin with EDTA for 10 minutes to release MSCs. Scaffolds were removed, medium containing serum was added to neutralize the trypsin, and the tubes were centrifuged at 16,000xg for 5 minutes to form a cell pellet. All liquid was aspirated, being careful not to disturb the pellet, then all tubes were immediately placed in liquid nitrogen to flash freeze the samples for RNA isolation.

RT-PCR

All PCR work was performed at the molecular resource center (MRC) at the University of Tennessee Health Science Center (Memphis TN). RNA was isolated using a RNeasy mini-kit (Qiagen, Hilden, DE) according the manufacturer's protocol. RNA quality and quantity were measured using a Qubit fluorometer (Invitrogen, Grand Island, NY). After analysis, amplification was deemed necessary. All RNA was transcribed to cDNA using first strand cDNA kit (Roche, Penzberg, DE). TaqMan PreAmp master mix (Invitrogen, Grand Island, NY) was used to amplify the cDNA. Separate PCR master mixes for each gene were then made with custom designed primers (Integrated DNA Technologies, Coralville, IA) for Collagen III, Decorin, Osteocalcin, and Aggrecan, as shown in Table 1. All primers were designed for rat genes and hypoxanthine-guanine phosphoribosyltransferase (HGPRT) was selected as the best reference gene. All samples plus master mixes were plated out and run for rt-PCR in a Light Cycler 480 (Roche Applied Sciences, Penzberg, DE). After PCR was complete, data was analyzed for relative changes to TCP using the delta delta C_t method[27].

Table I. PCR Primers Design

Gene	Gene Name	Accession Number	Sequence
Collagen type III	Col3A1	NM_032085.1	5'-tcccctggaatctgtgaatc-3' (forward)
			5'-tgagtcgaattggggagaat-3' (reverse)
Decorin	Dcn	NM_024129.1	5'-ctccgagtggtgcagtgtt-3' (forward)
			5'-gcaatgttgtgtcaggtgga-3' (reverse)
Osteocalcin	Bglap	M23637.1	5'-cattactgaccgctccttcc-3' (forward)
			5'-cgcatagcctgtgattttca-3' (reverse)
Aggrecan	Acan	NM_022190.1	5'-aatgggagccagcctacaac-3' (forward)
			5'-agaggcagagggactttcg-3' (reverse)

ECM Deposition

Extracellular matrix deposition on the scaffolds was quantified after 35 days in the mechanical bioreactor to characterize the coating. After the MSCs were removed from the scaffolds, each section was placed in a 1.5 mL microcentrifuge tube and 1 mL of a buffered 100 μg/mL proteinase-K (Promega, Madison, WI) solution was added to every tube. All samples were then placed in an oven at 60°C overnight to digest the ECM. The following day phenylmethanesulfonylfluoride (PMSF) was added to a final concentration of 5mM to inhibit the proteinase-K. All samples were homogenized using a sonic dismembrator and aliquots were removed for analysis. One aliquot was used to test for cell number through DNA quantification (Picogreen green assay, Invitrogen, Grand Island, NY). Another aliquot was used to measure the glycosaminoglycan (GAG) content (National Diagnostics, Atlanta, GA) through an alcian blue precipitation

reaction[28,29]. The last aliquot was used to quantify collagen content through the detection of the amino acid hydroxyproline (HYP)[30,31]. All volumes were carefully recorded for normalization during analysis.

Histology

Histology was performed at the University of Alabama-Birmingham Center for Metabolic Bone Disease. After scaffolds had been cultured in the mechanical bioreactor and ECM had been deposited across the scaffolds, one FB STIM and one FB+OB STIM scaffold was removed from the chamber and frozen. Samples were then fixed in 10% Neutral Buffered Formalin for at least 24 hours, then transferred to 70% ethanol (EtOH) for complete fixation. All the samples were dehydrated through cycles of 80% EtOH x1, 95% EtOH x2, and 100% EtOH x4 then three changes of xylene prior to the infiltration solution, 95% methyl methacrylate (MMA) and 5% dibutyl phthalate (DBP). Infiltration solutions for all the samples were refreshed every 3 days, for a total of 4 changes. After infiltration, the samples were embedded on edge in a solution composed by 95% MMA and 5% DBP with 0.25% perkodox as the initiator. The samples were then exposed to UV light for polymerization. The fully polymerized (plasticized) sample blocks were trimmed (noting which end was the bone side) and cut to obtain 5 μm thin sections through the longitudinal axis. There were four stains used including 1) Methylene Blue and Basic Fuchsin, 2) Goldner's Trichrome stain, 3) Toluidine Blue stain, and 4) Von Kossa stain. Stained sections were then observed and by light microscopy and captured images were analyzed using BioQuant Osteo II Software (Nashville, TN).

Statistics

The data was collected and averaged. The GAG and HYP were normalized to DNA and error was propagated[32]. Two-way ANOVA with respect to stretching and scaffold region with Holm-Sidak post-hoc test was performed on the necessary groups at a significance level of $\alpha=0.05$ using SigmaStat statistical software. For PCR data, after calculating the relative change and propagating error, two-way ANOVA was performed on relative changes with respect to scaffold region.

RESULTS

This preliminary study has three main objectives: (1) to determine gene activation of rat stem cells on the different deposited ECM coatings on the scaffold through rt-PCR, (2) to characterize the deposited ECM by measuring collagen and GAG content with hydroxyproline and alcian blue methods, respectively, (3) to visually evaluate the deposited ECM coating on the scaffolds using histology.

RT-PCR

Gene activation of rat MSCs seeded on the mechanically-stimulated scaffolds was measured using RT-PCR. Tendon-specific, bone-specific, and fibrocartilage-specific genes were selected for analysis. Collagen type III, decorin, osteocalcin, and aggrecan were measured. Collagen III is the second most common collagen type in tendon[3,33,34] and is also present in bone. Decorin is the primary proteoglycan found in tendon[33,34]. Osteocalcin is upregulated during bone formation[35]. Aggrecan is the primary proteoglycan in cartilaginous tissues[3]. Figure 3 shows the relative MSC gene activation on the tendon, bone, and transition regions of the scaffold compared to the MSCs cultured on TCP. These data represent activated tissue-specific genes in the MSCs after

24 hours of exposure to the ECM coated scaffolds. This PCR data does not represent how mechanical strain affected gene activation during ECM deposition on the scaffolds, but how the MSCs react to the mechanically-stimulated ECM deposited coating on the scaffolds. All four genes were upregulated compared to the TCP control. There were no significant differences between any of the experimental groups, shown in Figure 3, due to the high variance in the data. In general, the stretching had a slightly larger impact on the osteoblast region ECM compared to the fibroblast region ECM with respect to collagen and aggrecan. It was also observed that full scaffold mechanical stimulation, FB+OB STIM, produces a change in deposited ECM to increase MSC collagen activation and decrease mineralization activation compared to FB STIM scaffolds. When the OB region is stimulated in the FB+OB STIM scaffolds, there were indications of decreased MSC decorin expression compared to the FB STIM scaffolds. The two different mechanical conditioning treatments did not produce a significant difference in MSC aggrecan expression between groups but both were greater compared to the TCP control.

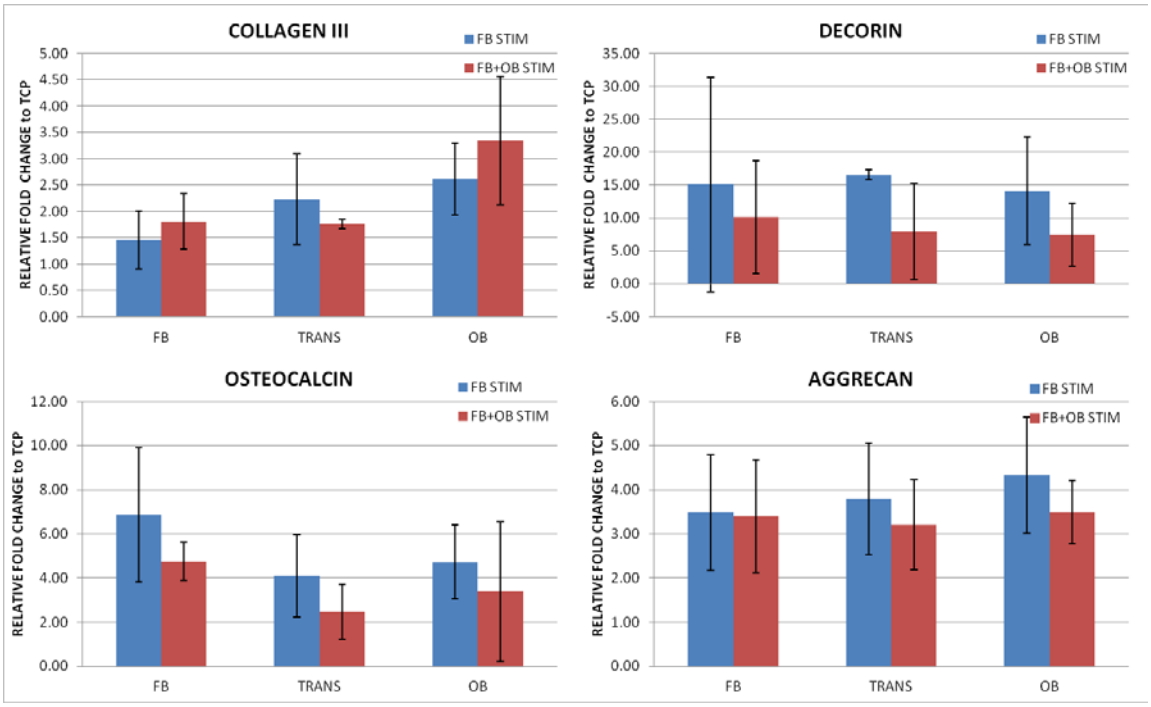

FIGURE 3. Mean relative fold change with standard deviations of gene activation in MSCs exposed to ECM depositions on scaffolds with mechanical stimulation compared to MSCs on tissue culture plastic. Generally, the ECM deposited on the FB+OB STIM scaffolds increased activated genes for collagen production, decreased mineralization, decreased tendon specific GAG, and no change in fibrocartilage activation compared to FB STIM scaffolds.

ECM Deposition

The ECM deposited on the scaffolds was characterized after removal of the MSCs with regards to GAG and HYP deposition which was normalized to DNA. The FB STIM scaffolds were strained with a center clamp in the transition zone of the scaffolds. Therefore, while stretching, no cells could grow under the clamp. After 21 days, the clamp was removed to allow cells to infiltrate this transition area for the remaining 14 days. While some cells were present in the transition area after 35 days, there was a significant decrease in cell number compared to the FB+OB STIM scaffolds. Generally there was more OB DNA than FB DNA on the scaffolds. Comparing the GAG/DNA for

the OB and FB, the different stimulation regimes did not significantly affect ECM deposition. However, there was a significant increase in the GAG/DNA deposition for the FB STIM scaffolds compared to FB+OB STIM scaffolds within the transition region. A similar trend appeared in the HYP/DNA data. The two different stretching regimes did not significantly affect ECM when comparing between individual regions of the scaffold. FBs were found to deposit significantly more collagen per cell than the OB.

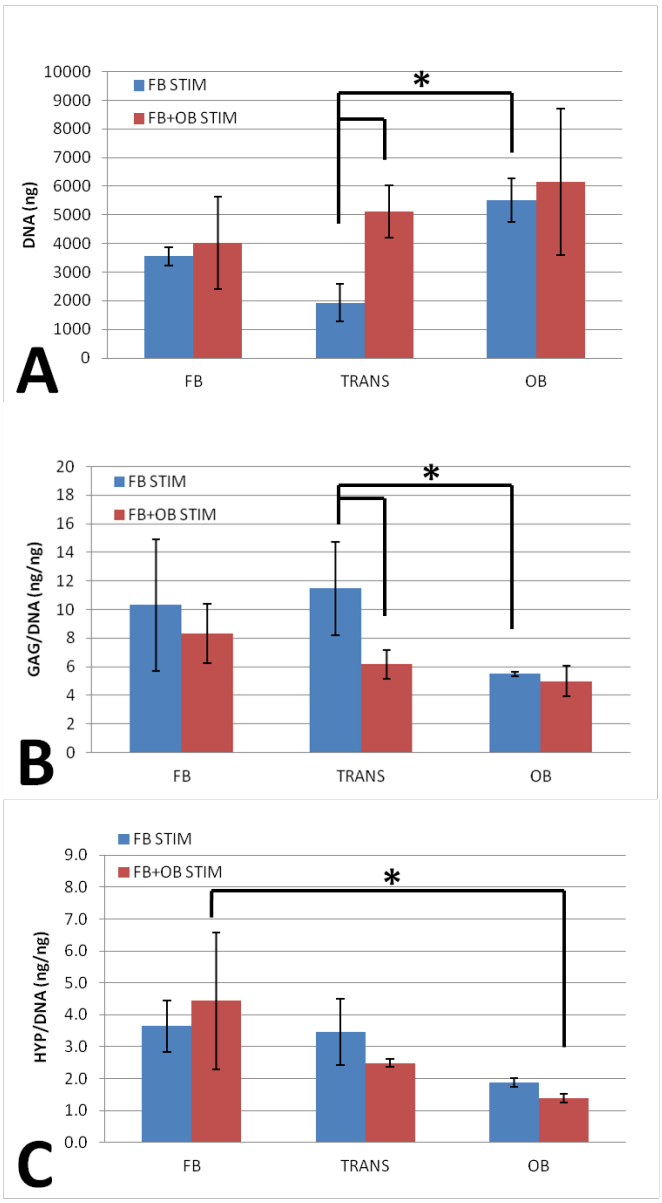

FIGURE 4. Characterization of ECM deposited on the scaffolds after 35 days of stimulation in the mechanical bioreactor. A) Mean DNA values ± standard deviation. B) GAG/DNA values ± standard deviation. C) Mean HYP/DNA values ± standard deviation. *Groups are statistically different at $p<0.05$.

Histology

Figure 5 shows a collage of histology slides from the four stains used on the FB STIM scaffold sections. Each image shows the thick ECM layer that was deposited on the surface of the scaffolds. Similar sections of the scaffold were selected for comparison between stains. Each image is a stitched composite of approximately fifty single frames at 10x magnification. Methylene blue and goldner trichrome stained the ECM the most intensely. Within the FB and OB regions a thick ECM layer was found with predominately highly aligned collagen and embedded cells as seen in Figure 6. The ECM deposition can be seen directly in contact with the PLA fibers of the scaffold. In some locations, the ECM layer was observed to be physically pulled away from the fibers. This ECM observation was potentially caused during the handling and histological processing of the scaffolds. Also, the majority of the ECM deposition occurred at the surface of the fabric layer. There was evidence of cell penetration and collagen deposition deeper within the fabric weave in a few isolated occurrences. There was also a noticeable absence of deposited ECM within the transition area of the FB STIM scaffold due to the presence of the center clamp during stimulation. Upon more detailed examination there was no noticeable mineralization in the von kossa or trichome staining and no fibrocartilage ECM deposition in the scaffold coating from these medium and mechanical stimulation conditions.

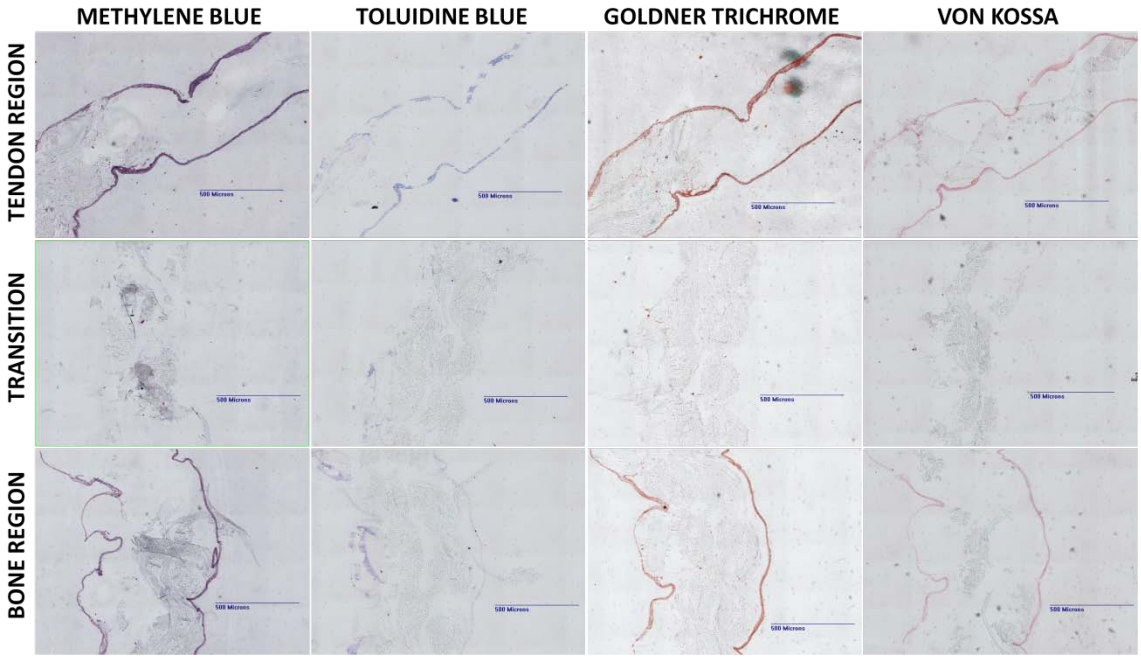

FIGURE 5. Histological staining of FB STIM scaffolds. The four stains are listed in columns and the scaffold sections are listed in the rows. The fibroblast "tendon" region stained for the most ECM and little to no mineralization. The center transition was positioned under a clamp for 21 days had little observed matrix deposition. The ECM layer is mostly highly aligned collagen seemed to stain more intensely in the FB region of the scaffold compared to the OB region. Mineral staining for early tissue calcification was not observed in the ECM coating. The scale bar in each image is 500 microns.

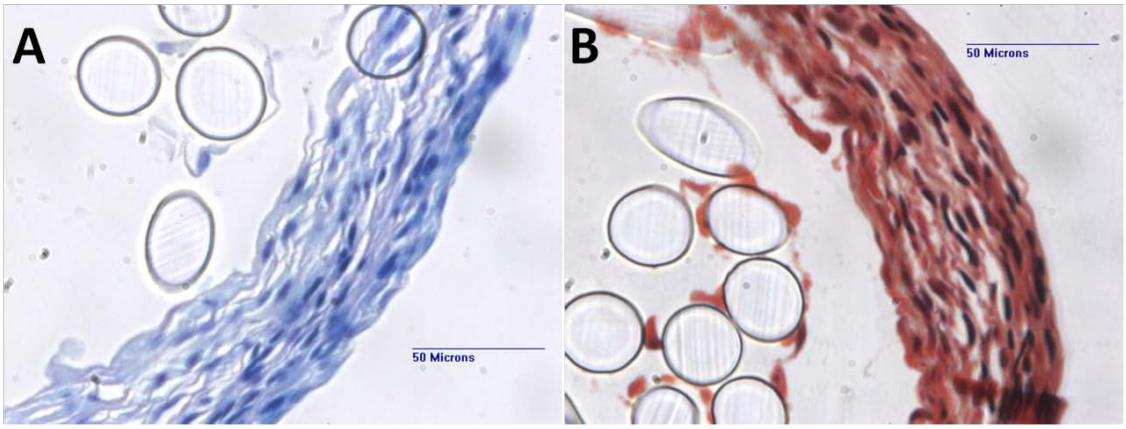

FIGURE 6. Higher magnification (40x) of the collagenous ECM coating on the FB+OB STIM scaffolds. (A) Toluidine blue stain of the ECM coating between the OB and transition regions and (B) Goldner trichrome stain of the ECM coating between the FB and transition region. Both images demonstrate multiple layers of highly aligned collagen and high cell numbers. Image B also indicates a lack of fibrocartilage and mineral staining. ECM can be observed in direct contact with the PLA fibers of the scaffold, and seems to have been physically separated during specimen slide preparation.

Figure 7 shows the collagen from the FB+OB STIM scaffolds. More intense and uniform staining of the ECM coating across the entire scaffold is shown in these conditions. As with the FB STIM, methylene blue and goldner trichrome stained the ECM the most intensely, but toluidine blue and von kossa were more intense on the FB+OB STIM scaffolds. ECM deposition in the transition region is intact due to the absence of the center clamp during stimulation. The transition images in Figure 7 show a dense cluster on the left side of the scaffold. This cluster is an indicator thread used to mark the midpoint of the scaffold. Since the thread was easily identified in each image, this location was selected as the locale of the transition comparisons. As with the FB STIM scaffolds, the ECM coating consists of a thick ECM layer of mostly highly aligned collagen with embedded cells. Most of the coating is on the surface. No observed mineralization or fibrocartilage was found in the ECM of the study conditions.

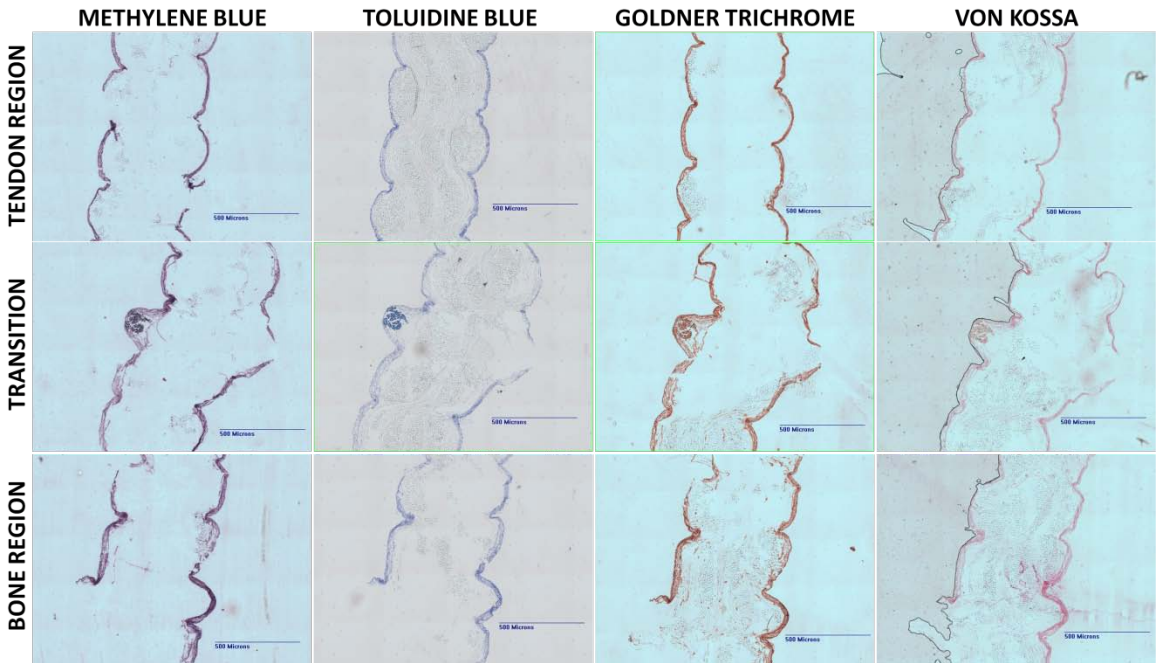

FIGURE 7. Histological staining of FB+OB STIM scaffolds. The four stains are listed in columns and the scaffold sections are listed in the rows. Similar scaffold sections were selected to compare ECM staining. ECM deposition was uniform on the surface of the fabrics for each section, including the transition region. The dense cluster on the left side of the transition region is an indicator thread used to mark the midpoint of the scaffold and was an easy target for selecting a comparable location. Collagen was highly aligned over the entire scaffold in the direction of the tensile strain. Little to no mineralization staining for any portion of the scaffold was observed under these study conditions. The scale bar in each image is 500 microns.

DISCUSSION

This study investigated the feasibility of generating a tissue-specific coating on a degradable scaffold for tendon-to-bone repair. The coating is formed by culturing fibroblasts and osteoblasts on separate regions of the scaffold and allowing these cells to deposit ECM. The tissue-specific ECM is further enhanced by applying mechanical stimulation to the scaffolds and cells over 35 days in culture during ECM deposition. This methodology is founded on the hypothesis that specific ECM can direct cells at the injury site to regenerate the tissues necessary for enthesis repair[36].

Biomaterial based scaffolds alone have been used in the past to repair injured ligaments at the bony interface in the ACL[37-40]. For example, polyester terepthalate (PET) scaffolds had promising short term functional results, however long term incorporation into the surrounding tissue failed[37,41]. ECM based scaffolds like small intestinal submucosa (SIS) and acellular dermal matrices (ACDM) are also being used clinically to aid in tendon repair[42-44]. These materials have shown very good tissue integration and injury site remodeling, but these ECM products have much lower mechanical properties than natural tendon or bone[42-44]. Therefore, a combination of a biomaterial based scaffold to achieve short term mechanical stability with an ECM based coating to help integrate into the surrounding tissue may provide better clinical outcomes. Specific ECM based components are powerful tools in tissue engineering because they can provide signals to the body's cells to regenerate or repair the damaged site[36]. Mechanical stimuli can be applied to the cells *in vitro* to create a more mimetic ECM coating on the scaffold potentially promoting faster scaffold/tissue integration.

Previous studies using mechanical bioreactors have shown that constructs with cell deposited collagen and ECM have increased mechanical strength properties compared to static culture [25], although reported conditions of how to apply the mechanical stimulation within the bioreactors widely vary. Strain magnitude, strain rate, number of cycles, cycle frequency, and rest durations can all affect the how the cells respond, and there is no consensus on the best parameter combination[18]. The optimal combinations of these parameters are almost certainly specific to the cell types and scaffold being used. Deng et al. reported using static strain to condition dermal fibroblasts on aligned PGA fibers[24]. Histology showed collagen alignment compared to

non-strained substrates and mechanical strength was greatly increased[24]. However, culture time was 18 weeks which may be too long for a practical therapy. Cyclic strain may produce results faster that static strain but can be dependent upon the strain profile. Riboh et al. demonstrated with primary tendon cells, continuous cyclic strain decreased cell proliferation, where as intermittent cyclic strain increased cell proliferation and increased total collagen production[23]. Johsi et al. varied cyclic strain parameters and found that ultimate tensile strength of their constructs was highest with relatively low cycle frequency and low strain magnitudes of 2.5%. They found that cell viability remained high for the entire study but no ECM characterization was reported[25]. Multiple studies have shown increases in tendon-specific markers with mechanical stimulation. Butler et al. and Abousleiman et al. showed increases in collagens type I and type III with direct stimulation of MSCs [6,18]and Yang et al. showed the same behavior in primary tendon fibroblasts using various stretching regimes[21]. The stimulation regime used in this study was chosen from average values of parameters described in the literature. The chosen stretching protocol is a good starting point for how mechanical stimulation can affect the scaffolds. Because of the number of variables associated with mechanically straining seeded scaffolds, there are future research opportunities to fully optimize the stretching protocol for our cell types and scaffolds.

Our cultured scaffolds demonstrated that collagen became aligned during cyclic stimulations and cell viability remained high throughout the study. There was no detectable mineralization in the ECM coating medium. While any potential *in vitro* calcification deposited was not expected to be mature hydroxyapatite, it was expected to see some calcium staining with the Von Kossa stain in the OB region of the scaffold[45].

Because the scaffolds used in our experiments are co-cultured with FB and OB, the osteogenic components were decreased to prevent FB ECM calcification. A study by Alverez-Perez et al. reported no *in vitro* mineralization of MSC deposited ECM on polycaprolactone (PCL) nanofibers when osteogenic medium was not used and positive mineralization when osteogenic medium was used[46]. It may have been the case that osteogenic signals were not strong enough. While preferential mineralization in the OB region compared to FB region would have been appreciated, the focus of this work was to modify deposited ECM through mechanical stimulation for a tendon-to-bone repair construct.

Even with the current mechanical stimulation parameters, an increase in tissue specific gene activation in MSCs was observed compared to a TCP control. Increases in collagen III, decorin, osteocalcin, and aggrecan activation were all expressed more due to the bioreactor conditioned coating. In a study by Sadr et al, MSC bone specific genes were activated more when exposed to cell deposited ECM compared to scaffolds alone similar to our findings[47]. There are also examples of gradients of ECM based coatings on synthetic scaffolds that can spatially upregulate gene activation across the scaffold[48,49]. When comparing actual deposited ECM on the scaffold to our previous tendon/bone scaffolds the mechanical conditioning produced a 575-720% increase in FB collagen deposition and 250-300% in OB deposition compared to static co-culture conditions (REF submissions). There was also an increase of 8-34% in FB GAG deposition and a decrease of 14-30% in OB GAG deposition (REF). This suggests that the mechanical conditioning causes more fibrous deposition in OBs and tendon like behavior in the FB.

In conclusion, we have designed and built a mechanical bioreactor that can apply different strains on a scaffold for different cell types to produce a more mimetic tissue specific coating. It was observed that stretching regimes in the bioreactor can affect the deposited ECM coating on the scaffold and tissue specific genes respond positively to the tissue specific ECM coatings compared to tissue culture plastic. Future work will focus on optimizing the stretching protocol for the deposited ECM coatings and evaluate the tissue specific coating in a functional tendon-to-bone animal model.

ACKOWLEDGEMENTS / FUNDING

We would like to thank Synthasome, Inc for generous donations of X-repair PLA fabric, William Taylor Ph.D, Felicia Waller, and Loren Rose at the University of Tennessee-Health Sciences Center Molecular Resource Center for help with RT-PCR, and Patty Lott at University of Alabama-Birmingham Center for Metabolic Bone Disease for histology work.

This project was funded by the DOD PRORP- USAMRMC W81XWH-10-1-0768 grant and by the Biomaterials Applications of Memphis (BAM) Laboratories in the Biomedical Engineering Department at the University of Memphis.

REFERENCES

1. Zhang X, Bogdanowicz D, Erisken C, Lee NM, Lu HH. Biomimetic scaffold design for functional and integrative tendon repair. J Shoulder Elbow Surg;21(2):266-77.

2. Wang IE, Shan J, Choi R, Oh S, Kepler CK, Chen FH, Lu HH. Role of osteoblast-fibroblast interactions in the formation of the ligament-to-bone interface. J Orthop Res 2007;25(12):1609-20.

3. Benjamin M, Milz S, Bydder GM. Magnetic resonance imaging of entheses. Part 1. Clin Radiol 2008;63(6):691-703.

4. Dourte LM, Kuntz AF, Soslowsky LJ. Twenty-five years of tendon and ligament research. J Orthop Res 2008;26(10):1297-305.

5. Cooper JA, Lu HH, Ko FK, Freeman JW, Laurencin CT. Fiber-based tissue-engineered scaffold for ligament replacement: design considerations and in vitro evaluation. Biomaterials 2005;26(13):1523-32.

6. Abousleiman RI, Reyes Y, McFetridge P, Sikavitsas V. Tendon tissue engineering using cell-seeded umbilical veins cultured in a mechanical stimulator. Tissue Eng Part A 2009;15(4):787-95.

7. Lu HH, Jiang J. Interface tissue engineering and the formulation of multiple-tissue systems. Adv Biochem Eng Biotechnol 2006;102:91-111.

8. Lu HH, Subramony SD, Boushell MK, Zhang X. Tissue engineering strategies for the regeneration of orthopedic interfaces. Ann Biomed Eng 2010;38(6):2142-54.

9. Yang PJ, Temenoff JS. Engineering orthopedic tissue interfaces. Tissue Eng Part B Rev 2009;15(2):127-41.

10. Zhang YY, He YJ, Bharadwaj S, Hammam N, Carnagey K, Myers R, Atala A, Van Dyke M. Tissue-specific extracellular matrix coatings for the promotion of cell proliferation and maintenance of cell phenotype. Biomaterials 2009;30(23-24):4021-4028.

11. Smith L, Xia Y, Galatz L, Genin G, Thomopoulos S. Tissue-engineering strategies for the tendon/ligament-to-bone insertion. Connective tissue research;53(2):95-105.

12. Spalazzi JP, Dagher E, Doty SB, Guo XE, Rodeo SA, Lu HH. In vivo evaluation of a tri-phasic composite scaffold for anterior cruciate ligament-to-bone integration. Conf Proc IEEE Eng Med Biol Soc 2006;1:525-8.

13. Spalazzi JP, Dagher E, Doty SB, Guo XE, Rodeo SA, Lu HH. In vivo evaluation of a multiphased scaffold designed for orthopaedic interface tissue engineering and soft tissue-to-bone integration. J Biomed Mater Res A 2008;86(1):1-12.

14. Spalazzi JP, Doty SB, Moffat KL, Levine WN, Lu HH. Development of controlled matrix heterogeneity on a triphasic scaffold for orthopedic interface tissue engineering. Tissue Eng 2006;12(12):3497-508.

15. Jiang T, Kumbar SG, Nair LS, Laurencin CT. Biologically active chitosan systems for tissue engineering and regenerative medicine. Curr Top Med Chem 2008;8(4):354-64.

16. Chamay A, Tschantz P. Mechanical influences in bone remodeling. Experimental research on Wolff's law. J Biomech 1972;5(2):173-80.

17. Woo SL, Abramowitch SD, Kilger R, Liang R. Biomechanics of knee ligaments: injury, healing, and repair. J Biomech 2006;39(1):1-20.

18. Butler DL, Hunter SA, Chokalingam K, Cordray MJ, Shearn J, Juncosa-Melvin N, Nirmalanandhan S, Jain A. Using functional tissue engineering and bioreactors to mechanically stimulate tissue-engineered constructs. Tissue Eng Part A 2009;15(4):741-9.

19. Moon du G, Christ G, Stitzel JD, Atala A, Yoo JJ. Cyclic mechanical preconditioning improves engineered muscle contraction. Tissue Eng Part A 2008;14(4):473-82.

20. Altman GH, Horan RL, Martin I, Farhadi J, Stark PR, Volloch V, Richmond JC, Vunjak-Novakovic G, Kaplan DL. Cell differentiation by mechanical stress. Faseb J 2002;16(2):270-2.

21. Yang G, Crawford RC, Wang JH. Proliferation and collagen production of human patellar tendon fibroblasts in response to cyclic uniaxial stretching in serum-free conditions. J Biomech 2004;37(10):1543-50.

22. Garvin J, Qi J, Maloney M, Banes AJ. Novel system for engineering bioartificial tendons and application of mechanical load. Tissue Eng 2003;9(5):967-79.

23. Riboh J, Chong AK, Pham H, Longaker M, Jacobs C, Chang J. Optimization of flexor tendon tissue engineering with a cyclic strain bioreactor. J Hand Surg Am 2008;33(8):1388-96.

24. Deng D, Liu W, Xu F, Yang Y, Zhou G, Zhang WJ, Cui L, Cao Y. Engineering human neo-tendon tissue in vitro with human dermal fibroblasts under static mechanical strain. Biomaterials 2009;30(35):6724-30.

25. Joshi SD, Webb K. Variation of cyclic strain parameters regulates development of elastic modulus in fibroblast/substrate constructs. J Orthop Res 2008;26(8):1105-13.

26. McCanless JD, Jennings LK, Cole JA, Bumgardner JD, Haggard WO. In vitro differentiation and biocompatibility of mesenchymal stem cells on a novel platelet releasate-containing injectable composite. J Biomed Mater Res A;100(1):220-9.

27. Livak KJ, Schmittgen TD. Analysis of relative gene expression data using real-time quantitative PCR and the 2(-Delta Delta C(T)) Method. Methods 2001;25(4):402-8.

28. Frazier SB, Roodhouse KA, Hourcade DE, Zhang L. The Quantification of Glycosaminoglycans: A Comparison of HPLC, Carbazole, and Alcian Blue Methods. Open Glycosci 2008;1:31-39.

29. Karlsson M, Bjornsson S. Quantitation of proteoglycans in biological fluids using Alcian blue. Methods Mol Biol 2001;171:159-73.

30. Stegemann H, Stalder K. Determination of hydroxyproline. Clin Chim Acta 1967;18(2):267-73.

31. Reddy GK, Enwemeka CS. A simplified method for the analysis of hydroxyproline in biological tissues. Clin Biochem 1996;29(3):225-9.

32. Beers Y. Introduction to the Theory of Error. Reading: Addison-Wesley Publishing Co.; 1957. 26-36. p.

33. Moffat KL, Wang IN, Rodeo SA, Lu HH. Orthopedic interface tissue engineering for the biological fixation of soft tissue grafts. Clin Sports Med 2009;28(1):157-76.

34. Amadio PC. Tendon and Ligament. In: Cohen IK, Diegelmann RF, Lindblad WJ, editors. Wound Healing: biochemical and clinical aspects. Philadelphia: W. B. Saunders Company; 1992. p 384-395.

35. Beresford JN, Gallagher JA, Poser JW, Russell RG. Production of osteocalcin by human bone cells in vitro. Effects of 1,25(OH)2D3, 24,25(OH)2D3, parathyroid hormone, and glucocorticoids. Metab Bone Dis Relat Res 1984;5(5):229-34.

36. Farach-Carson MC, Wagner RC, Kiick KL. Extracellular Matrix: Structure, Function, and Applications to Tissue Engineering. In: Bronzino JD, editor. Tissue Engineering and Artificial Organs. Boca Raton: CRC Press; 2006.

37. Guidoin R, Poddevin N, Marois Y, King MW, Belanger AY, Stroman P, Cronier B, Delagoutte JP, Maynard D, Benichoux R and others. Mechanisms of Failure for Anterior Cruciate Ligament Prostheses Implanted in Humans - a Retrospective Analysis of 79 Surgically Excised Explants. Polymers & Polymer Composites 1995;3(2):79-97.

38. Seitz H, Lang S, Marlovits S, Mousavi M, Kolonja A. Repair of the anterior cruciate ligament - a morphological study in sheep. Medizinische Welt 1998;49(12):610-617.

39. Seitz H, Marlovits S, Schwendenwein I, Muller E, Vecsei V. Biocompatibility of polyethylene terephthalate (Trevira (R) hochfest) augmentation device in repair of the anterior cruciate ligament. Biomaterials 1998;19(1-3):189-196.

40. Jenny JY, Jenny G, Daubresse F. Replacement of the Anterior Cruciate Ligament with Three Different Dacron Prostheses. International Orthopaedics 1991;15(1):23-28.

41. Guidoin MF, Marois Y, Bejui J, Poddevin N, King MW, Guidoin R. Analysis of retrieved polymer fiber based replacements for the ACL. Biomaterials 2000;21(23):2461-2474.

42. Derwin KA, Baker AR, Spragg RK, Leigh DR, Iannotti JP. Commercial extracellular matrix scaffolds for rotator cuff tendon repair. Biomechanical, biochemical, and cellular properties. J Bone Joint Surg Am 2006;88(12):2665-72.

43. Aurora A, McCarron J, Iannotti JP, Derwin K. Commercially available extracellular matrix materials for rotator cuff repairs: state of the art and future trends. J Shoulder Elbow Surg 2007;16(5 Suppl):S171-8.

44. Ricchetti ET, Aurora A, Iannotti JP, Derwin KA. Scaffold devices for rotator cuff repair. Journal of Shoulder and Elbow Surgery 2012;21(2):251-265.

45. Bonewald L, Harris S, Rosser J, Dallas M, Dallas S, Camacho N, Boyan B, Boskey A. von Kossa staining alone is not sufficient to confirm that mineralization in vitro represents bone formation. Calcified tissue international 2003;72(5):537-547.

46. Alvarez Perez MA, Guarino V, Cirillo V, Ambrosio L. In vitro mineralization and bone osteogenesis in poly(epsilon-caprolactone)/gelatin nanofibers. J Biomed Mater Res A;100(11):3008-19.

47. Sadr N, Pippenger BE, Scherberich A, Wendt D, Mantero S, Martin I, Papadimitropoulos A. Enhancing the biological performance of synthetic polymeric materials by decoration with engineered, decellularized extracellular matrix. Biomaterials;33(20):5085-93.

48. Seidi A, Ramalingam M, Elloumi-Hannachi I, Ostrovidov S, Khademhosseini A. Gradient biomaterials for soft-to-hard interface tissue engineering. Acta biomaterialia;7(4):1441-1451.

49. Wang X, Wenk E, Zhang X, Meinel L, Vunjak-Novakovic G, Kaplan D. Growth factor gradients via microsphere delivery in biopolymer scaffolds for osteochondral tissue engineering. Journal of controlled release : official journal of the Controlled Release Society 2009;134(2):81-90.

CHAPTER 5: PLANNED *IN VIVO* ANIMAL MODEL

Originally outlined in the awarded grant was an *in vivo* animal model planned to evaluate the effectiveness of tissue ingrowth and attachment of a tendon-bone tissue engineered scaffold in a rabbit tibial tendon-bone interface. This animal study had a total of 14 rabbits with 4 groups: mechanically-stimulated cultured ECM scaffolds, static cultured ECM scaffolds, scaffolds only, and reattached tendon. Surgeries were performed on 13 of 14 rabbits with 6 of 13 unexpectedly fracturing legs in less than 72 hours, leading to the termination of the study. These planned studies were based on published articles[38] and approved by proper IACUC and ACURO channels at University of Tennessee, University of Memphis, and USAMRMC. As such, we had no additional funds available to repeat a potential modified animal study to re-evaluate the ECM coated scaffolds. Therefore, a replacement study of gene activation of MSCs was performed to evaluate the function of the mechanically stimulated tissue specific scaffolds as outlined in Chapter 4.

THE UNIVERSITY of TENNESSEE UT
HEALTH SCIENCE CENTER

Institutional Animal Care & Use Committee
910 Madison Avenue, Suite 650
Memphis, TN 38163
Phone: (901) 448-3904
Fax: (901) 448-5222

MEMORANDUM:

TO: Dr. Richard Smith, Project Director

FROM: Mary Frances Braslow, Administrator-IACUC
Corresponding Secretary, Animal Care and Use Committee

SUBJECT: Animal Research Protocol Number **1988**
"Enhanced Soft Tissue Attachment and Fixation using a Mechanically Stimulated Cytoselective Tissue Specific Extracellular Matrix Coating"

DATE: March 29, 2011

Your protocol for animal experimentation has been **approved.** Please reference the protocol number in the appropriate space on the Animal Requisition form when ordering animals for use on this protocol.

An amended protocol should be submitted any time significant changes are made in the protocol, especially those involving a change of species, anesthesia, and/or procedures that may be considered stressful for the animal. All animal research protocols will be reviewed annually. At the appropriate time, you will be requested to verify, update, or inactivate this protocol.

The committee appreciates your conscientious cooperation in this very important program.

IACUC:032911:mfb

CHAPTER 6: CONCLUSIONS

In the scaffolds selection study in chapter 2 we determined that the BioTape scaffold had low mechanical strength and degraded before we could quantify ECM deposition. The degradable PLA fabric scaffold was able to provide good mechanical strength, while still allowing for high cell viability and deposition of collagen and GAG. The non-degradable PET fabric had similar mechanical properties, cell viability, and ECM deposition characteristics as the PLA scaffold. However between the two, the degradable biomaterial is a better choice because it allows for replacement with natural tissue as is degrades.

In chapter 3, we determined that with fluorescence cell tracking we are able to seed the PLA scaffold in co-culture to make a tendon-specific region and a bone-specific region on the scaffold. We also found a co-culture media formulation of alpha-MEM + 10% fetal bovine serum + 1x antibiotic/antimycotic+ 3 mM beta-glycerophosphate + 25 μg/mL of ascorbic acid to ECM deposition with low fibroblast mineralization and still provide for osteoblast mineralization. We also determined that a transition region is formed that has collagen and GAG amounts between the fibroblast and osteoblast regions.

In chapter 4, we successfully applied two different strains to a single scaffold to stimulate the tendon-region and osteoblast-region differently. The ECM that was deposited on the scaffolds was affected by the different stretching regimes. There were higher cell numbers and higher collagen to GAG ratio on scaffolds where both regions were stimulated. Tissue specific stem cell gene activation was increased on the mechanically stimulated scaffolds compared to tissue plastic.

We have demonstrated new protocols and methodologies to seed and characterize scaffolds for tendon-to-bone tissue engineering. Also a novel custom dual strain bioreactor was designed and developed for use in this project. These new technologies and methodologies will provide opportunities for future investigations and improvements in the tendon-to-bone repair research.

CHAPTER 7: RECOMMENDATIONS FOR FUTURE WORK

The first recommended action is to evaluate the mechanically stimulated tissue specific scaffolds in a functional animal model. I would recommend a model similar the one outlined in chapter 5 but with modifications. It is possible to re-do the study with a more proximal bone tunnel in tibia to reduce mid-bone stresses. The other recommendation is to perform the model with smaller scaffolds or use the same scaffolds in a slightly larger animal model other than rabbit. This would reduce the bone tunnel needed for a rabbit tibia or allow for a larger tunnel in a bigger tibia of a different animal.

I would recommend additional and more tissue specific assays to understand the deposition of tissue specific ECM on the scaffolds. We have demonstrated ECM deposition of collagen and GAG on the scaffolds. It would be an advantage to measure more specific changes in ECM deposited over the scaffold. This would allow us understand how to modify and improve our methods of cell seeding, media formulation, and stretching regimes of the scaffolds. These more specific assays could include more advance direct quantification through ELISA, PCR, or other assays and imaging through immunohistochemistry and histology.

It may be beneficial to move to duplicate characterizations we have learned with a different cell line, like primary cells. It may take a step towards a more mimetic assembly of tissue engineering parameters. There is certainly a large opportunity to experiment with different stretching protocols to alter the mechanical signal given to the cells during ECM deposition. We chose a single stretching protocol from the literature, and we have not fully optimized the stretching protocol for the cells we are using.

REFERENCES

1. Benjamin M, Milz S, Bydder GM. Magnetic resonance imaging of entheses. Part 1. Clin Radiol 2008;63(6):691-703.

2. Dourte LM, Kuntz AF, Soslowsky LJ. Twenty-five years of tendon and ligament research. J Orthop Res 2008;26(10):1297-305.

3. Spalazzi JP, Dagher E, Doty SB, Guo XE, Rodeo SA, Lu HH. In vivo evaluation of a multiphased scaffold designed for orthopaedic interface tissue engineering and soft tissue-to-bone integration. J Biomed Mater Res A 2008;86(1):1-12.

4. Yang PJ, Temenoff JS. Engineering orthopedic tissue interfaces. Tissue Eng Part B Rev 2009;15(2):127-41.

5. Smith L, Xia Y, Galatz LM, Genin GM, Thomopoulos S. Tissue-engineering strategies for the tendon/ligament-to-bone insertion. Connect Tissue Res;53(2):95-105.

6. Kuo CK, Marturano JE, Tuan RS. Novel strategies in tendon and ligament tissue engineering: Advanced biomaterials and regeneration motifs. Sports Med Arthrosc Rehabil Ther Technol;2:20.

7. Lu HH, Jiang J. Interface tissue engineering and the formulation of multiple-tissue systems. Adv Biochem Eng Biotechnol 2006;102:91-111.

8. Wang IE, Shan J, Choi R, Oh S, Kepler CK, Chen FH, Lu HH. Role of osteoblast-fibroblast interactions in the formation of the ligament-to-bone interface. J Orthop Res 2007;25(12):1609-20.

9. Aurora A, McCarron J, Iannotti JP, Derwin K. Commercially available extracellular matrix materials for rotator cuff repairs: state of the art and future trends. J Shoulder Elbow Surg 2007;16(5 Suppl):S171-8.

10. Ricchetti ET, Aurora A, Iannotti JP, Derwin KA. Scaffold devices for rotator cuff repair. Journal of Shoulder and Elbow Surgery 2012;21(2):251-265.

11. Zhang X, Bogdanowicz D, Erisken C, Lee NM, Lu HH. Biomimetic scaffold design for functional and integrative tendon repair. J Shoulder Elbow Surg;21(2):266-77.

12. Derwin KA, Codsi MJ, Milks RA, Baker AR, McCarron JA, Iannotti JP. Rotator cuff repair augmentation in a canine model with use of a woven poly-L-lactide device. J Bone Joint Surg Am 2009;91(5):1159-71.

13. Moffat KL, Wang IN, Rodeo SA, Lu HH. Orthopedic interface tissue engineering for the biological fixation of soft tissue grafts. Clin Sports Med 2009;28(1):157-76.

14. Cooper JA, Lu HH, Ko FK, Freeman JW, Laurencin CT. Fiber-based tissue-engineered scaffold for ligament replacement: design considerations and in vitro evaluation. Biomaterials 2005;26(13):1523-32.

15. Dormer NH, Berkland CJ, Detamore MS. Emerging techniques in stratified designs and continuous gradients for tissue engineering of interfaces. Ann Biomed Eng;38(6):2121-41.

16. Langer R, Vacanti JP. Tissue engineering. Science 1993;260(5110):920-6.

17. Lu HH, Subramony SD, Boushell MK, Zhang X. Tissue engineering strategies for the regeneration of orthopedic interfaces. Ann Biomed Eng 2010;38(6):2142-54.

18. Yang B, Zhang Y, Zhou L, Sun Z, Zheng J, Chen Y, Dai Y. Development of a porcine bladder acellular matrix with well-preserved extracellular bioactive factors for tissue engineering. Tissue Eng Part C Methods;16(5):1201-11.

19. Visser LC, Arnoczky SP, Caballero O, Kern A, Ratcliffe A, Gardner KL. Growth factor-rich plasma increases tendon cell proliferation and matrix synthesis on a synthetic scaffold: an in vitro study. Tissue Eng Part A 2010;16(3):1021-9.

20. Guidoin MF, Marois Y, Bejui J, Poddevin N, King MW, Guidoin R. Analysis of retrieved polymer fiber based replacements for the ACL. Biomaterials 2000;21(23):2461-2474.

21. Seitz H, Marlovits S, Schwendenwein I, Muller E, Vecsei V. Biocompatibility of polyethylene terephthalate (Trevira (R) hochfest) augmentation device in repair of the anterior cruciate ligament. Biomaterials 1998;19(1-3):189-196.

22. Jenny JY, Jenny G, Daubresse F. Replacement of the Anterior Cruciate Ligament with Three Different Dacron Prostheses. International Orthopaedics 1991;15(1):23-28.

23. Seitz H, Lang S, Marlovits S, Mousavi M, Kolonja A. Repair of the anterior cruciate ligament - a morphological study in sheep. Medizinische Welt 1998;49(12):610-617.

24. Sadr N, Pippenger BE, Scherberich A, Wendt D, Mantero S, Martin I, Papadimitropoulos A. Enhancing the biological performance of synthetic polymeric materials by decoration with engineered, decellularized extracellular matrix. Biomaterials;33(20):5085-93.

25. Derwin KA, Baker AR, Spragg RK, Leigh DR, Iannotti JP. Commercial extracellular matrix scaffolds for rotator cuff tendon repair. Biomechanical, biochemical, and cellular properties. J Bone Joint Surg Am 2006;88(12):2665-72.

26. Pauly S, Klatte F, Strobel C, Schmidmaier G, Greiner S, Scheibel M, Wildemann B. Characterization of tendon cell cultures of the human rotator cuff. Eur Cell Mater;20:84-97.

27. Deng D, Liu W, Xu F, Yang Y, Zhou G, Zhang WJ, Cui L, Cao Y. Engineering human neo-tendon tissue in vitro with human dermal fibroblasts under static mechanical strain. Biomaterials 2009;30(35):6724-30.

28. Chamay A, Tschantz P. Mechanical influences in bone remodeling. Experimental research on Wolff's law. J Biomech 1972;5(2):173-80.

29. Woo SL, Abramowitch SD, Kilger R, Liang R. Biomechanics of knee ligaments: injury, healing, and repair. J Biomech 2006;39(1):1-20.

30. Butler DL, Hunter SA, Chokalingam K, Cordray MJ, Shearn J, Juncosa-Melvin N, Nirmalanandhan S, Jain A. Using functional tissue engineering and bioreactors to mechanically stimulate tissue-engineered constructs. Tissue Eng Part A 2009;15(4):741-9.

31. Altman GH, Horan RL, Martin I, Farhadi J, Stark PR, Volloch V, Richmond JC, Vunjak-Novakovic G, Kaplan DL. Cell differentiation by mechanical stress. Faseb J 2002;16(2):270-2.

32. Yang G, Crawford RC, Wang JH. Proliferation and collagen production of human patellar tendon fibroblasts in response to cyclic uniaxial stretching in serum-free conditions. J Biomech 2004;37(10):1543-50.

33. Moon du G, Christ G, Stitzel JD, Atala A, Yoo JJ. Cyclic mechanical preconditioning improves engineered muscle contraction. Tissue Eng Part A 2008;14(4):473-82.

34. Garvin J, Qi J, Maloney M, Banes AJ. Novel system for engineering bioartificial tendons and application of mechanical load. Tissue Eng 2003;9(5):967-79.

35. Abousleiman RI, Reyes Y, McFetridge P, Sikavitsas V. Tendon tissue engineering using cell-seeded umbilical veins cultured in a mechanical stimulator. Tissue Eng Part A 2009;15(4):787-95.

36. Riboh J, Chong AK, Pham H, Longaker M, Jacobs C, Chang J. Optimization of flexor tendon tissue engineering with a cyclic strain bioreactor. J Hand Surg Am 2008;33(8):1388-96.

37. Joshi SD, Webb K. Variation of cyclic strain parameters regulates development of elastic modulus in fibroblast/substrate constructs. J Orthop Res 2008;26(8):1105-13.

38. Hashimoto Y, Yoshida G, Toyoda H, Takaoka K. Generation of tendon-to-bone interface "enthesis" with use of recombinant BMP-2 in a rabbit model. J Orthop Res 2007;25(11):1415-24.